

5G Network Planning under Service and EMF Constraints: Formulation and Solutions

Luca Chiaraviglio^(1,2), Cristian Di Paolo⁽²⁾, Nicola Blefari-Melazzi^(1,2)

1) Department of Electronic Engineering, University of Rome Tor Vergata, Rome, Italy,
email: luca.chiaraviglio@uniroma2.it, crisdp95@gmail.com, blefari@uniroma2.it

2) Consorzio Nazionale Interuniversitario per le Telecomunicazioni (CNIT), Italy

Abstract—We target the planning of a 5G cellular network under 5G service and ElectroMagnetic Fields (EMFs) constraints. We initially model the problem with a Mixed Integer Linear Programming (MILP) formulation. The pursued objective is a weighed function of next-generation Node-B (gNB) installation costs and 5G service coverage level from a massive Multiple Input Multiple Output (MIMO) system. In addition, we precisely model restrictive EMF constraints and we integrate scaling parameters to estimate the power radiated by 5G gNBs. Since the considered planning problem is NP-Hard, and therefore very challenging to be solved even for small problem instances, we design an efficient heuristic, called PLATEA, to practically solve it. Results, obtained over a realistic scenario that includes EMF exposure from pre-5G technologies (e.g., 2G, 3G, 4G), prove that the cellular planning selected by PLATEA ensures 5G service and restrictive EMF constraints. However, we demonstrate that the results are strongly affected by: *i*) the relative weight between gNB installation costs and 5G service coverage level, *ii*) the scaling parameters to estimate the exposure generated by 5G gNBs, *iii*) the amount of exposure from pre-5G technologies and *iv*) the adopted frequency reuse scheme.

Index Terms—5G Mobile Networks, 5G Network Planning, Base Station Deployment, Service and EMF constraints, EMF regulations



1 INTRODUCTION

The provisioning of the 5G service inevitably requires the installation of new 5G equipment, called next-generation Node-B (gNB), over the territory. The task of selecting and configuring the set of sites hosting 5G equipment is often referred as 5G cellular planning [1], a complex problem that involves costs, service coverage and ElectroMagnetic Field (EMF) constraints. In general, the planning of a cellular network is a critical step that has a huge impact on the CApital EXpenditures (CAPEX) costs incurred by the operator [2], as well as on the Quality of Service (QoS) perceived by users [3], [4]. From an operator perspective, network planning should minimize the costs for deploying new 5G sites and installing 5G equipment. In addition, the operator aims at maximizing the performance (e.g., throughput, delay) that is experienced by 5G User Equipment (UE).

Apart from economic and service goals, another important aspect that should be considered during the planning phase is the EMF exposure from 5G gNBs. More in depth, the radiation from 5G gNBs is a matter of strong debates among the population, including a supposed increase of exposure w.r.t. legacy technologies, as well as possible health effects associated with adoption of a wide range of frequencies (including mm-Waves). In this context, a clear causal-correlation between exposure levels from 5G gNBs operating below the limits defined by laws and emergence of health diseases has not been scientifically proven so far [5]. Therefore, it is of utmost importance to plan the network by ensuring EMF exposure constraints.

Under realistic settings, the planning problem is strongly affected by the regulations governing the EMF levels radiated by 5G equipment [6]. In general, many countries in the world ensure that the EMF levels radiated by 5G gNBs are lower than maximum values (often referred as

EMF limits) [7], which depend on the frequency exploited by the 5G gNB. Traditionally, international/federal bodies like International Commission on Non-Ionizing Radiation Protection (ICNIRP) and Federal Communications Commission (FCC) define EMF limits for all the cellular frequencies, including the ones used by 5G equipment [8], [9]. As a result, the constraints introduced by EMF regulations have to be carefully taken into account during the installation and then the operation of 5G equipment. Intuitively, the EMF constraints tend to limit the number of 5G sites installed over the territory and/or the amount of radiated power by each 5G gNB. Therefore, the EMF regulations have a large impact on the 5G gNB installation costs and the 5G service received by UE [1], [6], [10].

The picture is further complicated in different countries (such as Italy) [7], which introduce EMF regulations more restrictive than the ones defined by ICNIRP and FCC, on the basis of the application of a precautionary principle, in order to preserve the population from (still unknown) long-term health effects triggered by EMF exposure. Such restrictive rules include EMF limits strongly lower than the ones defined by ICNIRP/FCC [7], [11]. For example, ICNIRP regulations allow a maximum EMF exposure up to 61 [V/m] for frequencies above 2 [GHz], while this limit is decreased to only 6 [V/m] in the Italian EMF regulations that are applied in residential areas. In addition, other stringent rules include minimum distances between sensitive places (e.g., schools, hospitals public parks) and the installed 5G sites [12]. For example, a minimum distance of 100 [m] is applied in the city of Rome, an area of 1287 square kilometers inhabited by almost 3 million people.

As sketched in Fig. 1, the introduction of strict EMF limits strongly affects 5G network planning. For example, the

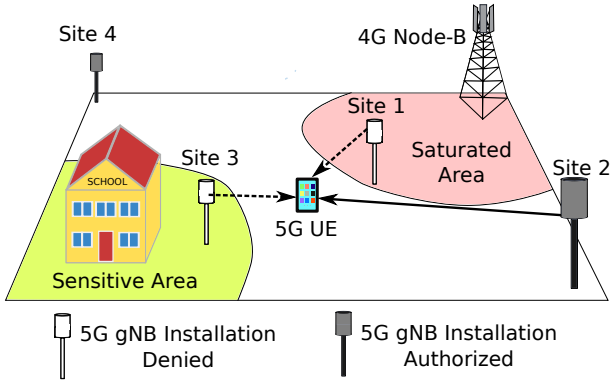


Fig. 1. The presence of sensitive areas and EMF saturation zones heavily impacts 5G cellular planning.

installation of new 5G sites is prevented within a minimum distance from the center of the sensitive area (e.g., the school in the figure). In addition, the enforcement of very low EMF limits tends to generate EMF saturation areas (e.g., the one shown on top right of the figure), where the EMF levels from pre-5G technologies are already close to the maximum limits. In such zones, therefore, the installation of new 5G sites is denied. As a result, the 5G sites have to be installed in other locations (i.e., not the optimal ones), thus further impacting the installation costs and the service level offered by the 5G network.

In this context, a natural question emerges: Is it possible to deploy a heterogeneous 5G network, while ensuring 5G service and restrictive EMF constraints? The ambitious goal of the paper is to tackle such interesting - and challenging - problem. Our innovative contributions can be summarized as follows. First, we take into account restrictive EMF regulations affecting the 5G planning phase, i.e., EMF limits stricter than ICNIRP/FCC ones, as well as enforcement of minimum distances between 5G sites and sensitive places. Second, we optimally model the 5G planning problem under service and EMF constraints, by assuming a 5G system based on massive Multiple-Input Multiple-Output (MIMO) functionalities. The presented problem integrates the widely used model of Marzetta [13] to compute the service level from a massive MIMO system, as well as the EMF point source described in International Telecommunication Union (ITU) K.70 recommendation [14], which is enriched by a set of scaling parameters to take into account temporal and statistical variations of radiated power from 5G MIMO systems with beamforming capabilities. We also show that the complete formulation falls within the class of Mixed Integer Linear Programming (MILP) problems and it is NP-Hard. Third, we design PLANNING ALGORITHM TOWARDS EMF EMISSIONS ASSESSMENT (PLATEA), a novel heuristic that is able to efficiently solve the 5G planning problem while ensuring adherence to strict EMF limits and 5G service for the set of pixels belonging to the area under consideration. Fourth, we evaluate PLATEA and two reference algorithms in a realistic scenario, whose parameters have been measured on the field (e.g., the EMF levels radiated by pre-5G sites already deployed in the scenario). Results prove that PLATEA outperforms the reference algorithms, by efficiently balancing between 5G gNB installation costs and

amount of 5G service coverage. In addition, we demonstrate that the scaling parameters used to compute the power radiated by 5G gNBs play a critical role in determining the selected planning and the EMF levels over the territory. Eventually, we show that the exposure levels generated by pre-5G technologies and the adopted frequency reuse factor have an impact on 5G planning.

To the best of our knowledge, previous works in the literature are focused on orthogonal aspects w.r.t the ones investigated in this paper. For example, Oughton *et al.* [2] target the solution of the 5G planning problem by means of techno-economic approaches, with little emphasis on the impact of EMF constraints. On the other hand, Matalatala *et al.* [15], [16] design heuristics targeting the reduction of the radiated power, EMF and/or specific absorption rate (SAR), without considering: *i*) the linearization of the problem constraints,¹ *ii*) the impact of the variation of the scaling parameters to compute the EMF levels from 5G gNBs, *iii*) the introduction of constraints to ensure a minimum distance between sensitive places and 5G gNBs, *iv*) the EMF and throughput evaluation over the whole territory (i.e., not only on single users). In this work, we show that both *ii*) and *iii*) are fundamental to determine the actual planning. In addition, we tackle both *i*) and *iv*) by adopting a pixel tessellation and a set of linearized constraints, which are included in an innovative formulation and a new algorithm.

The rest of the paper is organized as follows. Sec. 2 reviews the related work. The main building blocks of the considered 5G framework are highlighted in Sec. 3. Sec. 4 reports the problem formulation. The PLATEA algorithm is thoroughly described in Sec. 5. The scenario under consideration is detailed in Sec. 6. Results are analyzed in Sec. 7. Finally, Sec. 8 concludes our work.

2 RELATED WORKS

In the literature, different works investigate the cellular network planning problem under various angles, including e.g., application of Artificial Intelligence (AI)-based tools [17], identification of opportunities and challenges [18], optimal design response in smart grids [19], service-based network dimensioning [20]. Despite we recognize the importance of such previous works, none of them investigate the impact of EMF regulations on the planning.

Tab 1 reports the positioning of this paper w.r.t. [2], [15], [16], which we believe are the closest contributions to our work. More in depth, we consider the following features to classify [2], [15], [16] and our work: *i*) pursued goal(s) (e.g., cost reduction, power consumption reduction), *ii*) targeted 5G equipment type (e.g., generic gNBs, micro and macro gNBs), *iii*) modeled 5G service (e.g., SINR, network spectral efficiency, throughput, maximum coverage distance), *iv*) EMF features (e.g., temporal and statistical models, presence of exclusion zones in proximity to the gNB), *v*) considered EMF regulations (e.g., ICNIRP-based EMF limits, strict EMF limits, minimum site distance from sensitive places), *vi*) pursued methodology (e.g., model assessment, optimal formulation, heuristic) and *vii*) scenario complexity (e.g.,

1. The authors of [16] introduce an optimal formulation, which is however not linear w.r.t. the signal-to-noise ratio (SNR) computation, the electric field computation and the SAR computation.

TABLE 1
Work positioning w.r.t. the related literature.

Ref	Goal	5G Equip. Type	5G Service Metrics	EMF Features	EMF Regulations	Methodology	Scenario Complexity
[2]	Capacity and costs assessment	Micro & macro 5G gNBs	signal-to-interference plus noise ratio (SINR), network spectral efficiency	-	-	Model assessment	Hexagonal coverage layouts with 7 candidate sites, service area of few square kilometers, evaluation done on pixels.
[15]	Power consumption reduction, EMF exposure reduction	Generic gNBs operating at 3.7 [GHz]	Throughput, SINR	Presence of exclusion zones	Strict EMF limits	Heuristic	Dozens of candidate sites with irregular coverage layout, service area of several square kilometers, evaluation done on users (not on a pixel base).
[16]	Power consumption reduction, EMF exposure reduction, SAR exposure reduction, dose exposure reduction	Generic gNBs operating at 3.7 [GHz]	Throughput, SINR	Statistical models (with fixed parameters), presence of exclusion zones	ICNIRP-based EMF limits	Mixed Integer Non-Linear Programming (MINLP) optimization model, heuristic	Dozens of candidate sites with irregular coverage layout, service area of several square kilometers, evaluation done on users (not on a pixel base).
This work	Installation costs reduction, maximization of the number of served pixels	Micro & macro 5G gNBs	Throughput, minimum signal-to-interference ratio (SIR) threshold, maximum coverage distance	Temporal and statistical models (with variation of parameters), presence of exclusion zones	Strict EMF limits, minimum site distance from sensitive places	MILP optimization model, heuristic	Dozens of candidate sites with irregular coverage layout, service area of different square kilometers, evaluation done on pixels.

number of candidate sites, regular or irregular coverage layout, size of the service area, pixel or user evaluation).

Compared to [2], [15], [16], our work moves one step further by: *i)* explicitly targeting a weighed function of installation costs and service coverage, *ii)* considering a heterogeneous 5G network composed of micro and macro gNBs, in order to control the service level provided by micro gNBs and the one by macro gNBs, *iii)* precisely modeling multiple service metrics, including throughput, minimum SIR and maximum coverage distance, *iv)* performing the variation of the scaling parameters to compute the EMF, as well as including exclusion zones in proximity to the gNBs, *v)* integrating EMF regulations more restrictive than ICNIRP/FCC, both in terms of maximum limits and in terms of minimum distance between a 5G site and a sensitive place, *vi)* defining a linear formulation (MILP) and exploiting the linearized constraints to design the heuristic, *vii)* analyzing a large scenario composed of dozens of candidate sites with irregular coverage layouts, a service area in the order of different square kilometers, and service/EMF evaluations performed in each pixel of the territory.

3 BUILDING BLOCKS

The goal of the planning problem considered in this work is to install a 5G network of Non Standalone type for a single operator, in order to provide an enhanced Mobile BroadBand (eMBB) 5G service [21]. More specifically, the operator can install gNBs operating up to the 6 [GHz] band, which is the currently available option for implementing 5G in many countries in the world (including Italy). Basic coverage is provided by macro gNBs operating on sub-GHz frequencies, while micro gNBs operate on mid-

band frequencies to provide hot-spot capacity.² Clearly, micro and macro gNBs operate on different portions of the spectrum, which are also separated by those ones used by previous technologies and/or other operators from the same country.³

We then present the main building blocks that are integrated in our 5G framework, namely: *i)* the model to assess 5G performance, *ii)* the model to estimate EMF radiated by a set of gNBs and *iii)* the EMF regulations for the installation of 5G sites. In the following, we provide more details about each building block.

3.1 5G Performance Model

We adopt the widely known MIMO model of Marzetta [13] to evaluate the 5G performance for a set of installed gNBs. We refer to [13] for the details, while we report below the salient features. In brief, the model assumes that each site is equipped with arrays composed of a very large number of antenna elements. Moreover, the same power is radiated by all arrays operating at the same frequency.⁴ In the work of Marzetta [13], the number of antennas is higher than the number of users. Since the number of antennas is very large,

² 5G frequencies also include mm-Waves, which are however not being used in Italy at the time of preparing our study. Actually, the gNBs under installation include, in fact, the same equipment types assumed in this work (i.e., operating on sub-GHz and mid-band). Clearly, the adoption of equipment operating on mm-Waves may require service and/or EMF models potentially different than those ones employed in our work. This aspect is left as a future research activity, in parallel with the deployment of mm-Waves gNBs.

³ The investigation of spectrum sharing approaches, including e.g., carrier aggregation, channel bonding, licensed shared access, licensed assisted access, and/or location-based licensing [22], is left for future work.

⁴ In case the arrays operate with multiple power levels (e.g., due to different power budget settings), a different model has to be used. We leave the investigation of this aspect as future work.

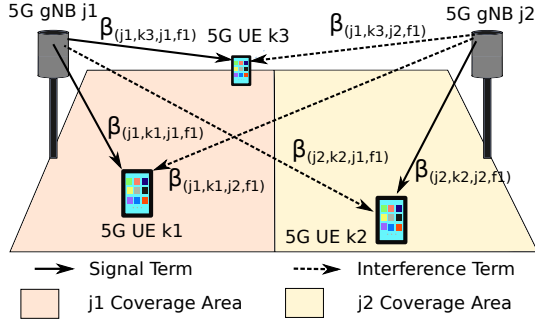


Fig. 2. Signal and interference terms in the 5G service model of [13] for a toy case scenario with two gNBs and three UEs.

the downlink SINR is dominated by the interference from neighboring gNBs rather than by the noise floor. More formally, the SIR of the k -th user served by l -th gNB operating on frequency f is defined as:⁵

$$S_{(k,l,f)} = \frac{\beta_{(l,k,l,f)}^2}{\sum_{j \neq l} \beta_{(l,k,j,f)}^2} \quad (1)$$

In the previous equation, the β terms are expressed as:

$$\beta_{(l,k,j,f)} = \frac{z_{(l,k,j,f)}}{D_{(k,l,f)}^{\gamma_f}} \quad (2)$$

where $D_{(k,l,f)}$ is the distance between 5G UE k and gNB operating on frequency f and installed at location l , γ_f is the path-loss exponent for frequency f and $z_{(l,k,j,f)}$ is a log-normal random variable modeling the shadow fading component, i.e., the quantity $10 \cdot \log_{10}(z_{(l,k,j,f)})$ (i.e., the shadow fading term in dB scale) is a distributed zero-mean Gaussian with a standard deviation σ_f^{SHAD} [13].

The β terms appearing in Eq. (1) are also sketched in the toy-case scenario of Fig. 2, which is composed by two gNBs and three UE. Intuitively, each 5G UE is served by a single gNB, while the other gNB contributes to the interference experienced by the 5G UE. It is important to remark that, in the downlink direction, the contributions of interference are solely due to the neighboring gNB, and not to the simultaneous transmissions to other UE in the same cell (e.g., terminals $k1$ and $k3$ in the figure), due to the fact that an Orthogonal Frequency-Division Multiplexing (OFDM) technology is assumed.

The downlink throughput received by user k from gNB installed at location l and operating on frequency f is then expressed as:

$$T_{(k,l,f)} = \frac{B_f \cdot \Gamma_f}{\epsilon_f^{\text{F-REUSE}}} \cdot \log_2(1 + S_{(k,l,f)}) \quad (3)$$

where: B_f is the gNB bandwidth, $\epsilon_f^{\text{F-REUSE}} \leq 1$ is a parameter governing the frequency reuse factor over frequency f

5. In the original model of [13] a set of gNBs operating at the same central frequency is assumed. In this work, instead, we consider a heterogeneous network composed of multiple tiers of gNBs operating at different frequencies. However, the extension of the model of Marzetta [13] to the multiple frequencies case is straightforward, as only gNBs operating on the same frequency have to be counted in the SIR computation of Eq. (1). Moreover, when spectrum-based approaches are introduced, the denominator has to include the interference terms from gNBs that compete on the same spectrum used by f .

TABLE 2
Expressions for the time-related parameters of [13].

Parameter	Expression
τ_f^{SLOT}	$\left[N_f^{\text{OFDM}} \cdot \left(\frac{1}{\Delta_f} \right) \right] + \delta_f$
τ_f^{PILOT}	$N_f^{\text{OFDM-PILOT}} \cdot \tau_f^{\text{SYMBOL}}$
τ_f^{SYMBOL}	$\frac{\tau_f^{\text{COHERENCE}}}{N_f^{\text{OFDM}}}$
τ_f^{USEFUL}	$\frac{1}{\Delta_f}$

(equal to 1 when a unity frequency reuse is adopted over frequency f), Γ_f is a shaping factor, formally expressed as:

$$\Gamma_f = \frac{(\tau_f^{\text{SLOT}} - \tau_f^{\text{PILOT}}) \cdot \tau_f^{\text{USEFUL}}}{\tau_f^{\text{SLOT}} \cdot \tau_f^{\text{SYMBOL}}} \quad (4)$$

where τ_f^{SLOT} is the slot duration over f , τ_f^{PILOT} is the pilot duration over f , τ_f^{SYMBOL} is the symbol interval over f and τ_f^{USEFUL} is the useful symbol duration over f . The expressions for τ_f^{SLOT} , τ_f^{PILOT} , τ_f^{SYMBOL} and τ_f^{USEFUL} are reported in Tab. 2, where N_f^{OFDM} is the number of OFDM symbols over f , Δ_f is the subcarrier spacing over f , δ_f is the cyclic prefix duration over f , $N_f^{\text{OFDM-PILOT}}$ is the number of OFDM symbols used for pilots over f and $\tau_f^{\text{COHERENCE}}$ is the coherence time over f .

Summarizing, the model of Marzetta [13] allows to compute the SIR and the maximum throughput for each UE, given the set of installed 5G gNBs and the UE-gNB association.

3.2 5G EMF Model

The second building block that is instrumental to our framework is the computation of the EMF that is received by a 5G UE from a 5G gNB. In the literature, different EMF models have been proposed to this purpose. We refer the interested reader to ITU-T K.70 recommendation [14] for an overview about the EMF models. In brief, the available options include point source models, synthetic models and full-wave models. In this work, we select the point source model, due to the following key properties: *i*) the actual EMF levels that are measured over the territory in the far-field region are typically lower than the ones estimated through the point source model of [14]. Therefore, when the EMF is computed through this model and the obtained level is below the maximum limit, the adherence to the limit is always guaranteed; *ii*) a linear set of constraints to compute the total EMF levels can be built when the model is integrated in our framework. Ensuring the linearity of the constraints is a desirable property, which, in fact, allows to reduce the complexity of both the optimal formulation and the designed heuristic. We also refer the interested reader to Appendix A for more considerations about the point source model.

More formally, the point source model allows to compute the power density $P_{(k,l,f)}$ that is received by UE k from a gNB located at site l and operating on frequency f .⁶ Clearly,

6. The power density metric is commonly used to characterize the level of exposure. Other exposure metrics include electric field, magnetic field and SAR. We refer the interested reader to [8] for an overview and comparison of the different exposure metrics.

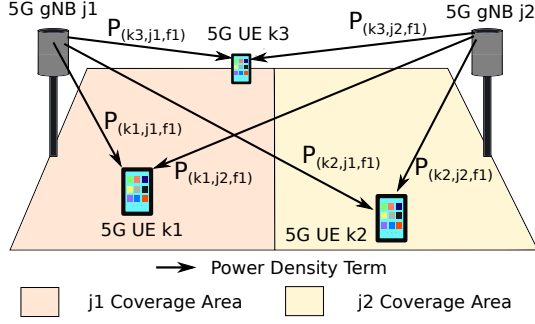


Fig. 3. Power density terms in the same toy case scenario of Fig. 2.

the distance $D_{(k,l,f)}$ between gNB l and UE k is assumed to be in the far-field region [14]. More formally, $P_{(k,l,f)}$ is expressed as:

$$P_{(k,l,f)} = \frac{\text{EIRP}_{(l,f)}}{4\pi \cdot D_{(k,l,f)}^2} \cdot F_{(k,l,f)} \quad (5)$$

where $\text{EIRP}_{(l,f)}$ is the Equivalent Isotropically Radiated Power (EIRP) from gNB operating on frequency f and located at site l and $F_{(k,l,f)} \leq 1$ is the normalized numeric gain over user k from an antenna installed at location l operating on frequency f . More in depth, $\text{EIRP}_{(l,f)}$ is formally expressed as:

$$\text{EIRP}_{(l,f)} = O_{(l,f)}^{\text{MAX}} \cdot \frac{\eta_f^{\text{GAIN}}}{\eta_f^{\text{LOSS}}} \quad (6)$$

where $O_{(l,f)}^{\text{MAX}}$ is the maximum output power for a gNB operating on frequency f and located at site l , η_f^{GAIN} is the transmission gain on frequency f , and η_f^{LOSS} is the transmission loss on frequency f .

By assuming the maximum achievable numeric gain $F_{(k,l,f)} = 1$ (as in [14]), Eq. (5) is simplified into:

$$P_{(k,l,f)} = \frac{\text{EIRP}_{(l,f)}}{4\pi \cdot D_{(k,l,f)}^2} \quad (7)$$

Given $P_{(k,l,f)}$, the electric field value $E_{(k,l,f)}$ is then expressed as:

$$E_{(k,l,f)} = \sqrt{P_{(k,l,f)} \cdot Z_0} \quad (8)$$

where Z_0 denotes the free space wave impedance.

Fig. 3 reports the power density terms $P_{(k,l,f)}$ in the same toy-case scenario of Fig. 2, which is composed by two gNBs operating at the same frequency f and three UEs. Actually, the total power density that is received by each UE is a linear combination of the single terms radiated by the two gNBs. For example, the total power density radiated over 5G UE $k1$ is simply equal to $P_{(k1,j1,f1)} + P_{(k1,j2,f1)}$. Note that, when considering the total electric field from multiple gNBs, a root mean square operator has to be applied. By considering the previous example, the total electric field that is radiated over UE $k1$ is equal to $\sqrt{E_{(k1,j1,f1)}^2 + E_{(k1,j2,f1)}^2}$. This operation introduces a non-linearity in the computation of the total exposure, which also generates non-linear constraints when binary variables are employed to select the set of sites that have to be installed out of the candidate ones. To overcome this issue, in this work we consider the computation of the total exposure through the power density

metric, which instead allows to preserve the linearity of the constraints.

When computing the exposure from a 5G gNB, a key role is played by the EIRP value appearing in Eq. (7). Clearly, the higher is the EIRP, the larger will be also the received power density $P_{(k,l,f)}$. This fact imposes to precisely estimate EIRP values that match real 5G gNB exposure patterns. In this context, two important elements that affect the EIRP values of a 5G gNB are the temporal variation and the statistical variation of the radiated power. We refer the interested reader to the International Electrotechnical Commission (IEC) standards [25], [26] for an overview about these aspects. In brief, the temporal variation is due to the fact that the number of 5G UE (and their traffic over the cellular network) exhibits a day-night pattern. Actually, the actual output power levels of the 5G gNB match this variation, with radiated power higher during the day and clearly lower during the night. On the other hand, the application of MIMO with beamforming features introduces strong variations in the radiated power over the territory, resulting in an exposure that is concentrated only to the zones where the served users are located. This issue is typically taken into account by solving statistical exposure models, which allow to compute spatially averaged radiated power values, as a consequence of the actual user distribution over the territory.

In this work, we take into account the aforementioned temporal and the statistical variability of the EIRP from 5G gNB by introducing two scaling parameters, denoted as $R_{(l,f)}^{\text{TIME}} \in (0, 1]$ and $R_{(l,f)}^{\text{STAT}} \in (0, 1]$, respectively. More in depth, $R_{(l,f)}^{\text{TIME}}$ captures the temporal variation of the radiated power (typically on a daily base), while $R_{(l,f)}^{\text{STAT}}$ models the statistical variation of exposure over the coverage area.⁷ As a result, the scaled EIRP from gNB installed at site l and operating on frequency f is computed as:

$$\text{EIRP}_{(l,f)}^{\text{TS}} = \text{EIRP}_{(l,f)} \cdot R_{(l,f)}^{\text{TIME}} \cdot R_{(l,f)}^{\text{STAT}} \quad (9)$$

In addition, let us introduce the power density $P_{(k,l,f)}^{\text{TS}}$ computed from $\text{EIRP}_{(l,f)}^{\text{TS}}$. By adopting Eq. (9) and the left-hand side of Eq. (7), $P_{(k,l,f)}^{\text{TS}}$ is formally expressed as:

$$P_{(k,l,f)}^{\text{TS}} = P_{(k,l,f)} \cdot R_{(l,f)}^{\text{TIME}} \cdot R_{(l,f)}^{\text{STAT}} \quad (10)$$

In this work, we use Eq. (7),(10) to characterize the level of exposure from a 5G gNB located at site l , operating on frequency f and radiating over UE k . Moreover, we demonstrate that the actual values of $R_{(l,f)}^{\text{TIME}}$ and $R_{(l,f)}^{\text{STAT}}$ have a crucial role in determining the level of exposure and consequently the set of gNBs that are installed over the territory.

3.3 5G EMF Constraints

We then consider the third building block of our framework, i.e., the integration of the 5G EMF constraints defined in the regulations. To this aim, Tab. 3 reports the set of regulations $R1$ - $R6$, which include ICNIRP guidelines ($R1$ - $R2$), Italian national regulations $R3$ - $R4$), and the local EMF regulations

⁷ The application of scaling parameters to compute realistic EIRP values is in line with the relevant literature involved in the 5G exposure modeling [26]-[29].

TABLE 3
Comparison across ICNIRP guidelines [8], [23], Italian regulations [11], [24] and Rome regulations [11], [12], [24].^{(a),(b),(c)}

ID	Name	Frequency range	Max. incident electric field	Max. incident power density L_f	Averaging time interval	Min. distance D^{MIN} from sensitive places
R1	ICNIRP 1998 Guidelines [23]	400 - 2000 [MHz] 2 - 300 [GHz]	$1.375 \cdot f^{0.5}$ [V/m] 61 [V/m]	$f/200$ [W/m ²] 10 [W/m ²]	6 [min] - up to 10 [GHz]	-
R2	ICNIRP 2020 Guidelines [8]	400 - 2000 [MHz] 2 - 300 [GHz]	$1.375 \cdot f^{0.5}$ [V/m] N/A	$f/200$ [W/m ²] 10 [W/m ²]	30 [min]	-
R3	Italian Regulation [11], [24] (General Public Areas)	3 - 3000 [MHz] 3 - 300 [GHz]	20 [V/m] 40 [V/m]	1 [W/m ²] 4 [W/m ²]	6 [min]	-
R4	Italian Regulation [11], [24] (Residential Areas)	0.1 [MHz] - 300 [GHz]	6 [V/m]	0.1 [W/m ²]	24 [h]	-
R5	Rome regulation [11], [12], [24] (General Public Areas)	3 - 3000 [MHz] 3 - 300 [GHz]	20 [V/m] 40 [V/m]	1 [W/m ²] 4 [W/m ²]	6 [min]	100 [m]
R6	Rome regulation [11], [12], [24] (Residential Areas)	0.1 [MHz] - 300 [GHz]	6 [V/m]	0.1 [W/m ²]	24 [h]	100 [m]

^(a) N/A stands for Not Applicable, meaning that the related quantity does not have to be taken into account when dealing with a compliance assessment.

^(b) The averaging time interval is the required amount of time to compute the average exposure levels that need to be compared against the maximum limit values.

^(c) f is the used frequency in MHz.

enforced in the city of Rome R5)-R6). For each regulation/guideline, the table reports: *i*) the frequency range relevant to 5G, *ii*) the maximum electric field limit for each frequency f , *iii*) the maximum power density limit L_f for each f , *iv*) the time interval to compute the average EMF that has to be compared against the limit value and *v*) the (eventual) minimum distance constraints that have to be ensured between the 5G installations and the sensitive places. As a side comment, we include in Tab. 3 the ICNIRP 1998 guidelines [23] and ICNIRP 2020 ones [8], due to the fact that the formers are still adopted in many countries in the world, while the latter are the up-to-date regulations which are going to be adopted in the forthcoming month/years, and hence in parallel with the deployment of 5G networks.

Several considerations hold by analyzing Tab. 3. First of all, R2) defines a power density limit and not a limit based on electric field strength, for all the frequencies between 2 [GHz] and 300 [GHz]. This fact further corroborates our choice for selecting the power density as the reference metric when performing the compliance assessment against the maximum limits. Second, the Italian regulations R3)-R4) are in general stricter than R1)-R2), both in terms of electric field and in terms of power density. Third, the Italian regulations in R3) and R4) further differentiate between general public areas (e.g., zones of the territory where the population is not continuously living) and residential areas (e.g., zones where people tend to live and/or work), respectively. Interestingly, R4) regulations are more restrictive than R3). Fourth, the city of Rome applies a minimum distance D^{MIN} from sensitive places in addition to the strict EMF limits defined in R3)-R4). Therefore, the regulations R5)-R6) further restrict R3)-R4). Fifth, the averaging time interval strongly varies across the different regulations, ranging from values of few minutes to 24 hours. This interval plays a crucial role in estimating the average EMF that has to be compared against the limit thresholds. Clearly, the lower is the time interval, the higher will be the influence of (possible) spikes on the average EMF. On the other hand, the higher is the time interval, the lower will be the impact of spikes on the average EMF. As a side comment, the instantaneous EMF field *can* be higher than the thresholds reported in Tab. 3. The actual metric

that is meaningful for comparison against the limit is in fact the average EMF over the time interval defined in each regulation.

After analyzing the EMF regulations, a natural question emerges: How to perform the compliance assessment w.r.t. the maximum limits when multiple Base Stations operating at different frequencies radiate the same area of territory? To answer this question, let us denote with $\sum_{l \in \mathcal{L}} P_{(k,l,f)}$ the composite power density that is radiated over UE k by all the Base Stations operating on frequency $f \in \mathcal{F}$, where \mathcal{F} is the set of frequencies in use. The compliance w.r.t. the limits is ensured over k if the following condition holds:

$$\sum_{f \in \mathcal{F}} \frac{\sum_{l \in \mathcal{L}} P_{(k,l,f)}}{L_f} \leq 1 \quad (11)$$

Clearly, the power density terms $P_{(k,l,f)}$ of Eq. (11) have to be computed as average values over the time intervals reported in Tab. 3. In addition, the actual EMF metric that is measured under practical conditions is the electric field strength $E_{(k,l,f)}$, which is then translated into power density $P_{(k,l,f)}$ by applying Eq. (8).

3.4 Summary and Next Steps

The model of Marzetta [13] is used to control the SIR and consequently the maximum downlink throughput provided to the UE. The point source model of ITU-T K.70 [14], integrated with scaling parameters that characterize the exposure from 5G gNB, is instead used to compute conservative estimation of power density. Finally, the limits defined by international/national bodies and local municipalities are used to ensure that the composite power density is lower than the thresholds. In addition, a minimum distance rule from sensitive places is ensured in accordance to the local regulation. In the next section, we join together these building blocks, in order to build an innovative formulation able to balance between gNBs installation costs and 5G service coverage level, while ensuring QoS and strict EMF constraints.

4 OPTIMAL 5G PLANNING FORMULATION

We divide our formulation in the following steps: *i*) preliminaries, *ii*) set definition, *iii*) constraint, variables and input parameters, *iv*) overall formulation.

4.1 Preliminaries

In the previous section we have provided the models to compute the service coverage and the power density for each UE in the scenario under consideration. In this section, we generalize these models by extending the evaluations from a sparse set of UE to a tessellation of non-overlapping squared pixels that fully cover the area under interest. More formally, the pixel is a small area of territory, in which similar propagation conditions are experienced. We refer the reader to Appendix B for a detailed discussion about the pixel tessellation.

Focusing then on the modelling of the EMF regulations, we assume to enforce the most restrictive ones, namely R5)-R6) of Tab. 3. Therefore, we distinguish between general public areas, residential areas and zones within the minimum distance from sensitive places. However, we point out that the other guidelines presented in Tab. 3 can be easily implemented in our framework by applying different limit thresholds and/or by setting the minimum distance D^{MIN} to zero.

4.2 Set Definition

Let us denote with \mathcal{P} the set of pixels under consideration. $\mathcal{P}^{\text{RES}} \subset \mathcal{P}$ and $\mathcal{P}^{\text{GEN}} \subset \mathcal{P}$ are the subsets of pixels in residential areas and in general public areas, respectively. Moreover, $\mathcal{P}^{\text{SENS}} \subset \mathcal{P}$ is the subset of pixels in sensitive areas. In addition, let \mathcal{L} be the set of candidate locations (sites) that can host 5G gNB equipment. Eventually, let \mathcal{F} be the set of frequencies that can be exploited by 5G gNBs.

4.3 Constraints, Variables and Input Parameters

We then detail constraints, variables and input parameters to our problem by adopting a step-by-step approach. We also refer the reader to Tab. 7 of Appendix C for the main notation that is adopted throughout the section.

5G Coverage and Service Constraints. We initially model the constraint that a pixel $p \in \mathcal{P}$ can be covered by a 5G gNB located in l only if the distance $D_{(p,l,f)}$ between the pixel and the installed gNB is lower than a maximum one, denoted with D_f^{MAX} , where f is the operating frequency of the 5G gNB installed in l . More formally, we have:

$$D_{(p,l,f)} \cdot x_{(p,l,f)} \leq D_f^{\text{MAX}} \cdot y_{(l,f)}, \quad \forall p \in \mathcal{P}, l \in \mathcal{L}, f \in \mathcal{F} \quad (12)$$

where $x_{(p,l,f)}$ is a binary variable, set to 1 if p is served by gNB operating on frequency f and located at l (0 otherwise). Moreover, $y_{(l,f)}$ is another binary variable, set to 1 if 5G gNB operating on frequency f is installed at location l (0 otherwise).

We then impose the constraint that each pixel p can be served by at most $N^{\text{SER}} \geq 1$ gNBs at the same time:⁸

$$\sum_{l \in \mathcal{L}} \sum_{f \in \mathcal{F}} x_{(p,l,f)} \leq N^{\text{SER}}, \quad \forall p \in \mathcal{P} \quad (13)$$

In the following, we impose that the SIR value in each pixel p that is served by a 5G gNB operating on frequency f has to be higher than a minimum value S_f^{MIN} . By adopting the SIR computation already introduced in Eq. (1),⁹ we have:¹⁰

$$\underbrace{\frac{\beta_{(l,p,l,f)}^2 \cdot y_{(l,f)}}{\sum_{l_2 \neq l \in \mathcal{L}} \beta_{(l,p,l_2,f)}^2 \cdot y_{(l_2,f)}}}_{\text{SIR } S_{(p,l,f)}} \geq \underbrace{S_f^{\text{MIN}}}_{\text{Min. SIR Threshold}} \cdot x_{(p,l,f)}, \quad \forall p \in \mathcal{P}, l \in \mathcal{L}, f \in \mathcal{F} \quad (14)$$

Clearly, the previous constraint is not linear, due to the optimization variables $y_{(l,f)}$ that appear on both the numerator and the denominator of the left-hand side, coupled with the presence of the $x_{(p,l,f)}$ variables on the right-hand side of the constraint. To solve this issue, we apply a linearization procedure. More in depth, we refer the reader to Appendix D for the details, while we report below the final outcomes. In brief, we replace Eq. (14) with the following linear constraints:

$$v_{(l,p,l_2,f)} \leq x_{(p,l,f)}, \quad \forall p \in \mathcal{P}, l \in \mathcal{L}, l_2 \in \mathcal{L}, f \in \mathcal{F} \quad (15)$$

$$v_{(l,p,l_2,f)} \leq y_{(l_2,f)}, \quad \forall p \in \mathcal{P}, l \in \mathcal{L}, l_2 \in \mathcal{L}, f \in \mathcal{F} \quad (16)$$

$$v_{(l,p,l_2,f)} \geq x_{(p,l,f)} + y_{(l_2,f)} - 1, \quad \forall p \in \mathcal{P}, l \in \mathcal{L}, l_2 \in \mathcal{L}, f \in \mathcal{F} \quad (17)$$

$$S_f^{\text{MIN}} \cdot \left[\sum_{l_2 \in \mathcal{L}} \frac{\beta_{(l,p,l_2,f)}^2}{\beta_{(l,p,l,f)}^2} \cdot v_{(l,p,l_2,f)} - x_{(p,l,f)} \right] \leq 1 \quad \forall p \in \mathcal{P}, l \in \mathcal{L}, f \in \mathcal{F} \quad (18)$$

where $v_{(l,p,l_2,f)} \in \{0, 1\}$ is a binary auxiliary variable.

Power Density Limits. We initially select the pixels that fall in the exclusion zones of the installed 5G gNBs and therefore are not subject to the EMF limits defined for the general public. More formally, we introduce the binary variable w_p , set to 1 if p is located inside an exclusion zone of an installed gNB (0 otherwise). In addition, input parameter $I_{(p,l,f)}^{\text{ZONE}}$ takes value 1 if pixel p is inside the exclusion zone of

8. Although multiple coverage from different gNBs is a desirable condition, the increase in the number of gNBs covering the same pixel may introduce side effects, like an increase in the handover rates for UE, which may dramatically decrease the perceived QoS [6]. Therefore, we introduce a constraint to control the number of gNBs serving the same pixel.

9. Since we have extended the evaluation from the single UE to the whole set of pixels, the k index of Eq. (1) is replaced with $p \in \mathcal{P}$.

10. The adopted SIR model assumes a flat terrain, i.e., without considering possible hills/valleys that can affect the SIR computation. Intuitively, a possible way to take into account the terrain elevation changes would be to exploit a gray-scale pixel map [30], with different shades representing different elevation value. We leave the investigation of this aspect as future work.

gNB operating on frequency f and located at l (0 otherwise). The value of w_p is then set through the following set of constraints:

$$w_p \geq I_{(p,l,f)}^{\text{ZONE}} \cdot y(l,f), \quad \forall p \in \mathcal{P}, l \in \mathcal{L}, f \in \mathcal{F} \quad (19)$$

$$w_p \leq \sum_{l \in \mathcal{L}} \sum_{f \in \mathcal{F}} I_{(p,l,f)}^{\text{ZONE}} \cdot y(l,f), \quad \forall p \in \mathcal{P} \quad (20)$$

More in depth, constraint (19) activates w_p if p is inside at least one exclusion zone of an installed gNB. On the other hand, constraint (20) forces w_p to 0 if p is outside the exclusion zones for all the installed gNBs.

In the following, we introduce the constraints to compute the power density received by pixel p over frequency f . Let us denote with input parameter $P_{(p,l,f)}^{\text{ADD}}$ the additional power density that is received by pixel p when a gNB operating on frequency f is installed in l . Let us denote with $P_{(p,f)}^{\text{ADD-TS}}$ the variable storing the additional power density for pixel p over f , which is computed from $P_{(p,l,f)}^{\text{ADD}}$ by applying the scaling factors $R_{(l,f)}^{\text{TIME}}$ and $R_{(l,f)}^{\text{STAT}}$. More formally, we include Eq. (10) to our problem, thus yielding:

$$P_{(p,f)}^{\text{ADD-TS}} = (1 - w_p) \sum_{l \in \mathcal{L}} P_{(p,l,f)}^{\text{ADD}} \cdot R_{(l,f)}^{\text{TIME}} \cdot R_{(l,f)}^{\text{STAT}} \cdot y(l,f) \quad \forall p \in \mathcal{P}, f \in \mathcal{F} \quad (21)$$

In the previous constraint, the term $(1 - w_p)$ ensures that a pixel falling inside the exclusion zone of an installed 5G gNB is not considered when the power density is evaluated against the limits. However, the presence of the term $(1 - w_p) \cdot y(l,f)$ makes Eq. (21) not linear. We then linearize it by: *i*) introducing the auxiliary variable $z_{(p,l,f)} \in \{0, 1\}$, and *ii*) replacing Eq. (21) with the following set of constraints:

$$z_{(p,l,f)} \leq (1 - w_p), \quad \forall p \in \mathcal{P}, l \in \mathcal{L}, f \in \mathcal{F} \quad (22)$$

$$z_{(p,l,f)} \leq y(l,f), \quad \forall p \in \mathcal{P}, l \in \mathcal{L}, f \in \mathcal{F} \quad (23)$$

$$z_{(p,l,f)} \geq y(l,f) - w_p, \quad \forall p \in \mathcal{P}, l \in \mathcal{L}, f \in \mathcal{F} \quad (24)$$

$$P_{(p,f)}^{\text{ADD-TS}} = \sum_{l \in \mathcal{L}} P_{(p,l,f)}^{\text{ADD}} \cdot R_{(l,f)}^{\text{TIME}} \cdot R_{(l,f)}^{\text{STAT}} \cdot z_{(p,l,f)} \quad \forall p \in \mathcal{P}, f \in \mathcal{F} \quad (25)$$

To give more insights, we demonstrate with a simple example that Eq. (24) is essential to correctly set $z_{(p,l,f)}$. Let us consider the following case: *i*) the pixel p is outside the exclusion zone, and hence $w_p = 0$, and *ii*) there is a gNB installed at location l operating at frequency f , and therefore $y(l,f) = 1$. When only (22)-(23) are considered (without (24)), a feasible solution in this case would be to set $z_{(p,l,f)} = 0$, which is not correct because the product $(1 - w_p) \cdot y(l,f)$ in the non-linear constraint (21) is equal to one in the same case. On the other hand, when (24) is introduced, $z_{(p,l,f)}$ is (correctly) set to 1.

In a similar way, we compute the additional total power density $P_{(p,f)}^{\text{ADD-NOTS}}$ that is received by pixel p on frequency f , without applying the scaling factors $R_{(l,f)}^{\text{TIME}}$, $R_{(l,f)}^{\text{STAT}}$. $P_{(p,f)}^{\text{ADD-NOTS}}$ is meaningful when p belongs to a general

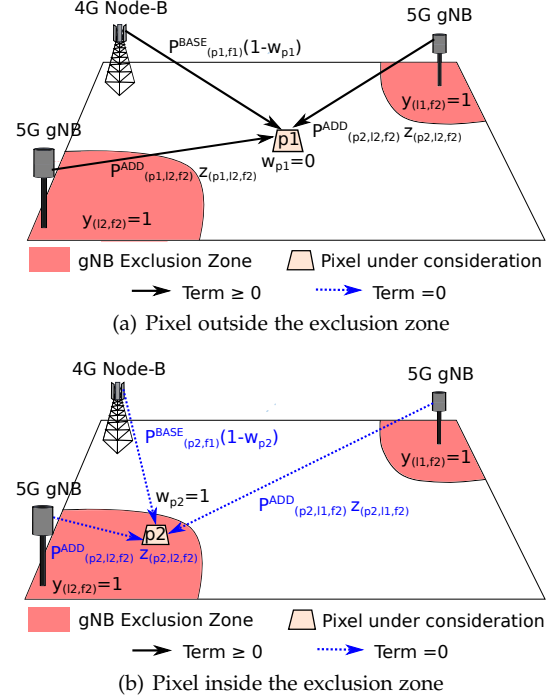


Fig. 4. Computation of the power density terms in a toy-case scenario that includes exclusion zones from the newly installed gNBs.

public area (e.g., $R5$ of Tab. 3). In this case, in fact, the scaling parameters are not applied.¹¹ Therefore, we have:

$$P_{(p,f)}^{\text{ADD-NOTS}} = \sum_{l \in \mathcal{L}} P_{(p,l,f)}^{\text{ADD}} \cdot z_{(p,l,f)}, \quad \forall p \in \mathcal{P}, f \in \mathcal{F} \quad (26)$$

We then impose the power density limit on residential areas, which has to be ensured for each pixel $p \in \mathcal{P}^{\text{RES}}$. More technically, we include the compliance assessment model of Eq. (11) in our problem, thus obtaining:

$$\sum_{f \in \mathcal{F}} \frac{P_{(p,f)}^{\text{BASE}} \cdot (1 - w_p) + P_{(p,f)}^{\text{ADD-TS}}}{L_f^{\text{RES}}} \leq 1, \quad \forall p \in \mathcal{P}^{\text{RES}} \quad (27)$$

where $P_{(p,f)}^{\text{BASE}}$ is the baseline power density over p from all the radio-frequency sources operating of frequency f and already installed in the scenario under consideration.

Finally, we impose the power density limit on general public areas, which has to be ensured for each pixel $p \in \mathcal{P}^{\text{GEN}}$, by introducing the following constraint:

$$\sum_{f \in \mathcal{F}} \frac{P_{(p,f)}^{\text{BASE}} \cdot (1 - w_p) + P_{(p,f)}^{\text{ADD-NOTS}}}{L_f^{\text{GEN}}} \leq 1, \quad \forall p \in \mathcal{P}^{\text{GEN}} \quad (28)$$

In order to clarify how the computation of the power density is governed by the optimization variables modelling the exclusion zones, Fig. 4 shows a graphical representation of $P_{(p,l,f)}^{\text{ADD}} \cdot z_{(p,l,f)}$ terms that appear in Eq. (25)-(26) as well as $P_{(p,f)}^{\text{BASE}} \cdot (1 - w_p)$ that are included in Eq. (27)-(28). More in depth, the considered toy-case scenario includes one legacy 4G Node-B already installed over the territory and two newly installed gNBs. Fig. 4(a) focuses on a pixel $p1$ outside

¹¹ A revision in the regulations may be introduced in the future in order to introduce scaling parameters also for general public areas.

the exclusion zones of the gNBs. By applying Eq. (19)-(20), it holds that $w_{p1} = 0$. Then, by applying constraints (22)-(24), it holds that: $z_{(p1,l1,f2)} = 1$, $z_{(p1,l2,f2)} = 1$. Consequently, the computation of the total power density in (27)-(28) will include the contributions from the newly installed gNBs as well as the already installed 4G Node-B. Therefore, the installation of the newly installed gNB is possible only if the EMF compliance assessment constraints (27)-(28) are ensured. On the other hand, Fig. 4(b) reports the power density terms when the considered pixel $p2$ falls inside the exclusion zone of a gNB. By applying Eq. (19)-(20),(22)-(24) it holds that: $w_{p2} = 1$, $z_{(p2,l1,f2)} = 0$, $z_{(p2,l2,f2)} = 0$. As a result, the power density terms $P_{(p2,l,f)}^{\text{ADD}} \cdot z_{(p2,l,f)}$ and $P_{(p2,f1)}^{\text{BASE}} \cdot (1 - w_{p2})$ are now set to zero. Therefore, the EMF compliance assessment constraints (27)-(28) are always ensured for $p2$.

Minimum Distance from Sensitive Places. We then introduce the distance constraints that are included in regulations R5)-R6) of Tab. 3. We remind that these constraints define a minimum distance between each installed 5G gNB and a sensitive place. More formally, we have:

$$D_{(p,l,f)} \cdot y_{(l,f)} \geq D^{\text{MIN}}, \quad \forall p \in \mathcal{P}^{\text{SENS}}, l \in \mathcal{L}, f \in \mathcal{F} \quad (29)$$

Site Constraints. In the following, we impose that each site location can host up to N^{MAX} gNB types operating at different frequencies. More formally, we have:

$$\sum_{f \in \mathcal{F}} y_{(l,f)} \leq N^{\text{MAX}}, \quad \forall l \in \mathcal{L} \quad (30)$$

In addition, we introduce the indicator parameter $I_{(l,f)}^{\text{FREQ}}$, taking value 1 if gNB of type f can be hosted at location l , 0 otherwise. Clearly, a gNB operating on frequency f can be installed at l only if the indicator parameter is 1. More formally, we have:

$$y_{(l,f)} \leq I_{(l,f)}^{\text{FREQ}}, \quad \forall l \in \mathcal{L}, f \in \mathcal{F} \quad (31)$$

Total Cost Computation. Finally, we compute the total costs for installing the 5G gNBs. To this aim, let us denote with parameter C_f^{EQUIP} the monetary costs of a 5G gNB equipment operating on frequency f . In addition, let us denote with parameter $C_{(l,f)}^{\text{SITE}}$ the site installation cost for a 5G gNB operating on frequency f and installed at location l . The total costs C^{TOT} for installing the new 5G gNBs are formally expressed as:

$$C^{\text{TOT}} = \sum_{l \in \mathcal{L}} \sum_{f \in \mathcal{F}} \left(C_f^{\text{EQUIP}} + C_{(l,f)}^{\text{SITE}} \right) \cdot y_{(l,f)} \quad (32)$$

4.4 Objective Function and Overall Formulation

We consider a multi-objective function that combines the total costs for installing the 5G gNBs (stored in variable C^{TOT}) and the number of pixels that are served by the installed 5G gNBs (stored in variables $x_{(p,l,f)}$). The two terms are properly taken into account by the weight factor $\alpha_{(l,f)}$ [EUR], which represents the per-pixel revenue by gNB operating on frequency f and located in l . More in depth, the $\alpha_{(l,f)}$ parameters have to be provided in input to our framework, and they can be estimated e.g., from the expected lifetime duration of a gNB installation, the zones that are served by the gNB, the projected increase

of users over the years, and/or a weighed function of the aforementioned terms. Interestingly, by varying the values of $\alpha_{(l,f)}$ over the set of locations \mathcal{L} and over the set of frequencies \mathcal{F} , the operator can control the installation costs and the coverage level over the territory.¹²

The complete OPTIMAL PLANNING FOR 5G NETWORKS UNDER SERVICE AND STRICT EMF CONSTRAINTS (OPTPLAN-5G) is formally expressed as:

$$\min \left(C^{\text{TOT}} - \sum_{p \in \mathcal{P}} \sum_{l \in \mathcal{L}} \sum_{f \in \mathcal{F}} \alpha_{(l,f)} \cdot x_{(p,l,f)} \right) \quad (33)$$

subject to:

$$\begin{aligned} \text{5G Coverage and Service:} & \quad \text{Eq. (12, 13), (15) - (18)} \\ \text{Power Density Limits:} & \quad \text{Eq. (19, 20), (22) - (28)} \\ \text{Min. Distance Constraint:} & \quad \text{Eq. (29)} \\ \text{Site Constraints:} & \quad \text{Eq. (30), (31)} \\ \text{Total Cost Computation:} & \quad \text{Eq. (32)} \end{aligned} \quad (34)$$

under variables: $C^{\text{TOT}} \geq 0$, $x_{(p,l,f)} \in \{0, 1\}$, $y_{(l,f)} \in \{0, 1\}$, $w_p \in \{0, 1\}$, $v_{(p,l,l2,f)} \in \{0, 1\}$, $z_{(p,l,f)} \in \{0, 1\}$.

Proposition 1. *The OPTPLAN-5G problem is NP-Hard.*

Proof. Let us consider a special case of the problem, where a single pixel is evaluated. Moreover, let us assume that this single pixel is covered if the gNB operating on frequency f is installed in l , i.e., $x_{(p,l,f)} = y_{(l,f)}$, $\forall l \in \mathcal{L}, f \in \mathcal{F}$.¹³ Let us also consider the possibility to install up to one gNB in each site, i.e., $N^{\text{MAX}} = 1$. Consequently, constraint (30) can be rewritten as:

$$\sum_{f \in \mathcal{F}} y_{(l,f)} \leq 1, \quad \forall l \in \mathcal{L} \quad (35)$$

Moreover, let us assume that the considered pixel is outside the exclusion zone of each installed gNB, i.e., $w_p = 0$. Consequently, $z_{(p,l,f)} = y_{(l,f)}$, $\forall l \in \mathcal{L}, f \in \mathcal{F}$. Moreover, we consider: *i)* the application of general public limits, i.e., the scaling parameters are not applied and *ii)* a relaxation of the power density constraints in (28) with no background power density (i.e., $P_{(p,f)}^{\text{BASE}} = 0, \forall f \in \mathcal{F}$) and the limit verification for each frequency in isolation w.r.t. the other frequencies. More formally, constraint (28) is replaced with the following one:

$$\sum_{l \in \mathcal{L}} P_{(p,l,f)}^{\text{ADD}} \cdot y_{(l,f)} \leq L_f^{\text{GEN}}, \quad \forall f \in \mathcal{F} \quad (36)$$

We then assume the maximization of the service coverage, which in our problem is equivalent to the maximization of the number of installed gNBs, weighted by $\alpha_{(l,f)}$. More formally, we have:

$$\max \sum_{l \in \mathcal{L}} \sum_{f \in \mathcal{F}} \alpha_{(l,f)} \cdot y_{(l,f)} \quad (37)$$

12. Other alternative formulations commonly adopted during the cellular planning phase include the minimization of the CAPEX costs under a given percentage of service coverage. However, this goal does not always guarantee problem feasibility. To overcome this issue, in this work we keep the service coverage in the objective function. As a result, our choice allows to preserve the problem feasibility on one side and to explore the impact of $\alpha_{(l,f)}$ on the obtained planning on the other one.

13. In this way, we assume that the pixel is within D^{MAX} distance from all the gNBs and that the minimum value of service throughput is equal to 0.

Algorithm 1 Pseudo-Code of PLATEA algorithm

Input: Parameters and sets defined in Tab. 7 of Appendix C, assumed to be available through global variables

Output: Variables $y, x, P^{\text{ADD-TS}}, P^{\text{ADD-NOTS}}, w, C^{\text{TOT}}$ for the best solution found

```

1: // Step 1: Initialization
2: num_f1_max =  $\sum_{l \in \mathcal{L}} I_{(f_1, l)}^{\text{FREQ}}$ ; // Max. number of installable  $f_1$  gNBs
3: num_f2_max =  $\sum_{l \in \mathcal{L}} I_{(f_2, l)}^{\text{FREQ}}$ ; // Max. number of installable  $f_2$  gNBs
4: best_obj = inf; // Best objective initialization
5:  $[y, x, P^{\text{ADD-TS}}, P^{\text{ADD-NOTS}}, w, C^{\text{TOT}}]$  = INITIAL_SOL(); // Initialization of solution variables
6: // Step 2: iteration over candidate deployments with frequency  $f_1$ 
7: for num_f1=1:num_f1_max do
8:   [flag_end x_curr, y_curr, pd_curr] = SELECT_BEST_SET_F1(num_f1); // Selection of the best deployment with
   num_f1 gNBs
9:   // Step 3: iteration over candidate deployments with frequency  $f_2$ 
10:  for num_f2=1:num_f2_max do
11:    if flag_end == false then
12:      sites_f2_comb = EXTRACT_SITES(num_f2, f2); // Extraction of the candidate deployments with
   frequency  $f_2$ 
13:      for sites_f2 in sites_f2_comb do
14:        [flag_check, y_curr, pd_curr] = INSTALL_CHECK(sites_f2, y_curr, pd_curr); // Based on Eq. (19), (20),
   (22) - (31)
15:        if flag_check == true then
16:          [x_curr] = ASSOCIATE_PIXELS(y_curr, x_curr); // Based on Eq. (12), (13), (15) - (18)
17:          curr_obj = COMPUTE_OBJ(x_curr, y_curr); // Based on Eq. (32), (33)
18:          if curr_obj < best_obj then
19:            best_obj = curr_obj;
20:             $[y, x, P^{\text{ADD-TS}}, P^{\text{ADD-NOTS}}, w, C^{\text{TOT}}]$  = SAVE_SOL(y_curr, x_curr, pd_curr); // Best Solution Saving
21:          end if
22:          if (ALL_SERVED(x_curr) == true) then
23:            flag_end = true; // All pixels served
24:          end if
25:          [x_curr, y_curr, pd_curr] = UNINSTALL(f2, x_curr, y_curr, pd_curr); // Revert changes for  $f_2$ 
26:        end if
27:      end for
28:    end if
29:  end for
30:  [x_curr, y_curr, pd_curr] = UNINSTALL(f1, x_curr, y_curr, pd_curr); // Revert changes for  $f_1$ 
31: end for

```

subject to: Eq. (35), Eq. (36); under variables: $y_{(l, f)} \in \{0, 1\}$. It is therefore trivial to note that the aforementioned formulation is the well-known GENERALIZED ASSIGNMENT PROBLEM (GAP), which is NP-Hard [31]. Since GAP is a special case of our problem, we can conclude that also OPTPLAN-5G is NP-Hard. \square

5 PLATEA ALGORITHM

Since the OPTPLAN-5G is NP-Hard, and therefore very challenging to be solved even for small problem instances, we design an efficient algorithm, called PLANNING ALGORITHM TOWARDS EMF EMISSION ASSESSMENT (PLATEA) to practically solve it. We base our solution on the following intuitions:

- 1) we apply a *divide et impera* approach, in which the complex planning problem is split into sets of subproblems. More in depth, since the different frequencies used in 5G have in general different goals (e.g., throughput maximization and/or coverage maximization), we exploit the gNB operating frequency as the main metric to split the original problem into smaller subproblems;
- 2) we restrict the exploration of the solution space by evaluating subsets among all the possible combinations of candidate deployments. However, we

introduce a parameter to control the exploration level of the combinations set;

- 3) we exploit the linear constraints introduced in the previous section to limit the computational complexity of PLATEA.

Alg. 1 reports the high-level pseudo-code of PLATEA. The source code of the algorithm is also available for download [32]. More in detail, we design PLATEA by assuming that two distinct frequencies f_1 and f_2 are exploited, with f_1 targeting throughput maximization and f_2 targeting coverage maximization.¹⁴ In order to ease the presented pseudo-codes, we adopt the following guidelines: *i*) the input parameters and sets defined in Tab. 7 of Appendix C are assumed to be available through global variables, and *ii*) the subscripts appearing in the parameters/variables are hindered. The algorithm then produces as output the selected deployment y , the pixel to gNB association x , the power density variables $P^{\text{ADD-TS}}, P^{\text{ADD-NOTS}}$, the exclusion

¹⁴ In our case, f_1 is a mid-band frequency, while f_2 is a sub-GHz frequency. These two sets of frequencies are the ones currently in use by 5G, while the exploitation of frequencies in the mm-Wave band is still at the early stage in many countries in the world. However, PLATEA may be easily generalized also to the case in which three types of frequencies (i.e., sub-GHz, mid-band, mm-Waves) are employed. We leave this aspect as future work.

Algorithm 2 Pseudo-Code of the SELECT_BEST_SET_F1 function

Input: num_f1 deployed gNBs with frequency f_1
Output: flag_end flag with installation status (false = installation successful, true = installation unsuccessful), temporary variables x_{best} , y_{best} , pd_{best}

```

1: best_obj=inf;
2: flag_end=true;
3: sites_f1_comb=EXTRACT_SITES(num_f1,f1); //
  Extraction of the candidate deployments
  with frequency f1
4: for sites_f1 in sites_f1_comb do
5:   [x_temp y_temp pd_temp]=INITIALIZE();
6:   [flag_check, pd_temp]=INSTALL_CHECK(sites_f1,
  y_temp, pd_temp); // Based on Eq. (19), (20),
  (22)-(31) with frequency f1
7:   if flag_check==true then
8:     flag_end=false;
9:     [x_temp]=ASSOCIATE_PIXELS(y_temp, x_temp);
  // Based on Eq. (12), (13), (15)-(18) with
  frequency f1
10:    temp_obj=COMPUTE_OBJ(x_temp, y_temp); //
  Based on Eq. (32), (33) with frequency f1
11:    if temp_obj < best_obj then
12:      best_obj=temp_obj;
13:      x_best=x_temp;
14:      y_best=y_temp;
15:      pd_best=pd_temp;
16:    end if
17:  end if
18: end for

```

zone variable w and the total installation costs C^{TOT} for the selected deployment.

We then describe the operations performed by PLATEA. Initially, the maximum number of installable gNB is computed (lines 2-3). In the following, all the variables are initialized to zero values by the INITIAL_SOL function (line 5). PLATEA then iterates over the possible candidate deployments with frequency f_1 (lines 7-31). In particular, the SELECT_BEST_SET_F1 function in line 8 retrieves the best solution found for each number of installable f_1 gNBs, starting from one up to the maximum number (line 7).

In the following, we provide more details about the SELECT_BEST_SET_F1 function, which is expanded in Alg. 2. The function requires as input the number of targeted gNBs to be installed, denoted as num_f1. Then, the function produces as output a flag (indicating if a feasible deployment has been found), as well as temporary variables storing the current set of installed f_1 gNBs, the current pixel to gNB association, and the current power density over the set of pixels. After initializing the routine variables (line 1-2), the function retrieves the possible combinations of f_1 gNBs, by running the EXTRACT_SITES routine (line 3). Since enumerating all the possible combinations is a challenging step in terms of computational requirements, we control the amount of generated combinations by assuming that up to num_f1 candidate deployments are randomly generated. Intuitively, when num_f1 is low, it is not meaningful to explore the whole space of combinations, since the number of served pixels will be in any case rather limited. On the other hand, we consider more combinations as num_f1 increases, since the impact on service coverage may be not

negligible in this case.

In the following (lines 4-18), the SELECT_BEST_SET_F1 function iterates over the set of selected combinations. In particular, the constraints about power density limits in Eq. (19), (20), (22)-(28), minimum distance from sensitive places in Eq. (29) and site constraints in Eq. (30)-(31) are checked over frequency f_1 . If the previous constraints are all met, the pixels are associated to the installed gNBs (line 9) and the objective function is evaluated (line 10). More in depth, the association of pixels in line 9 is performed by sequentially analyzing the set of installed gNBs and by associating each pixel while ensuring the 5G coverage and service constraints of Eq. (12),(13),(15)-(18) with frequency f_1 . Clearly, if the previous constraints are not met, the current pixel is not associated to the gNB under consideration. In addition, the computation of the objective function in line 10 exploits constraints Eq. (32),(33) with frequency f_1 . Eventually, the best solution is updated in lines 11-16.

When SELECT_BEST_SET_F1 is terminated, PLATEA performs lines 9-31 of Alg. 1. In particular, the algorithm iterates over the candidate deployments on frequency f_2 (line 10). Clearly, this step is performed only if a feasible candidate deployment over frequency f_1 has been found (line 11). In the following, the algorithm generates num_f2 combinations of f_2 gNBs (line 12), and then iterates over each candidate deployment (lines 13-27) in order to verify the constraints (line 14) and eventually to perform the gNB-pixel association (lines 15-16). The functions used in these steps are exactly the same adopted in Alg. 2, except from the adopted frequency, which is now set to f_2 . In the following, the objective function is evaluated (line 17), and the best solution is eventually updated (lines 18-21). The algorithm then stops evaluating further deployments if all the pixels have been served (line 22-24). Clearly, when passing between the evaluation of one deployment to the following one, the changes operated on the temporary variables are reverted to the previous state (lines 25,30).

Finally, we compute the computational complexity of PLATEA. The detailed breakdown of the complexity for the single functions is reported in Appendix. E, while here we report the salient features. In brief, the overall complexity of PLATEA is in the order of $\mathcal{O}(|\mathcal{P}| \times |\mathcal{L}|^5 \times |\mathcal{F}|)$.

6 SCENARIO DESCRIPTION

We consider as reference scenario the TMC neighborhood in Rome, Italy. The area under consideration, spanning over 2.47 [km²], is actually populated by more than 10000 inhabitants. We select the TMC neighborhood due to the following reasons: *i*) TMC includes residential areas and sensitive places (i.e., public parks, schools, churches, recreation centers); therefore, its territory is subject to very stringent EMF regulations (i.e., R6 regulation of Tab. 3), *ii*) the terrain is almost plain, i.e., there are not steep hills and/or large obstacles (apart from the buildings), which would otherwise affect the propagation conditions, *iii*) 5G coverage is not actually provided in the neighborhood, *iv*) pre-5G base stations are installed only outside the neighborhood, *v*) background information about pre-5G coverage and QoS levels experienced in TMC is already available in [6].



Fig. 5. TMC map with candidate locations for f_1 gNBs (orange pins) and for f_2 gNBs (blue pins).

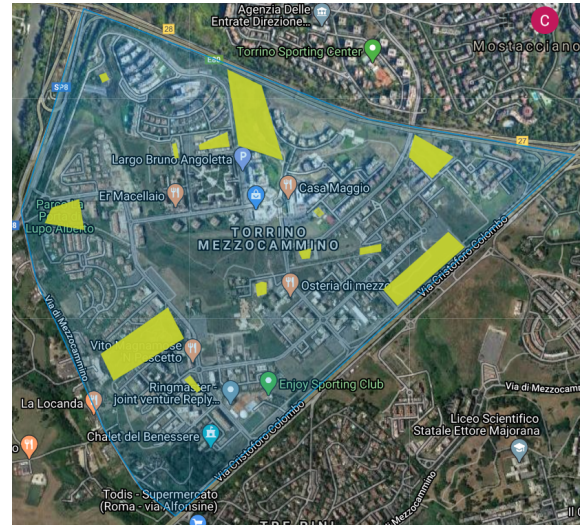


Fig. 6. TMC map with sensitive places highlighted in yellow.

We then focus on the set of frequencies \mathcal{F} that are employed by 5G gNBs. More in detail, we consider the exploitation of two distinct frequencies, namely $f_1 = 3700$ [MHz] and $f_2 = 700$ [MHz]. Both f_1 and f_2 have been recently auctioned to 5G operators in Italy [33]. Therefore, we expect that both f_1 and f_2 will be used by 5G equipment in the forthcoming years.¹⁵ In this work, we assume that f_1 is exploited by micro gNBs to provide hot-spot capacity, while the f_2 is employed by macro gNBs mainly for coverage. As a consequence, we differentiate f_1 and f_2 in terms of candidate sites, coverage distance, EMF values, 5G performance indicators and costs parameters.

In the following, we provide more details about the area under consideration, the set of pixels, the set of candidate gNBs and the set of sensitive places. To this aim, Fig. 5 reports: *i*) the TMC neighborhood (transparent blue area), *ii*) the set of locations \mathcal{L} that can host 5G gNBs (i.e., the union of blue and orange pins), *iii*) the subset of locations that can host f_1 gNBs (orange pins), and *iv*) the subset of locations that can host f_2 gNBs (blue pins). The selection of locations in *iii*) and *iv*) is driven by the following principles: *a*) installation of f_2 gNBs mainly on top of buildings, in order to maximize the coverage over the territory, *b*) installation of f_1 gNBs close to the zones where capacity is needed (along the roads and in proximity to the residential buildings). As a result, a total of $|\mathcal{L}| = 69$ candidate locations are taken into account in this work, thus leading to a total number of candidate deployments equal to 2^{69} .¹⁶

In the following, we move our attention to the set of

15. Apart from f_1 and f_2 , the auction of 5G frequencies in Italy included also a band at 26 [GHz] (i.e., close to mm-Waves) [33]. However, the 26 [GHz] frequency is intentionally left apart from this paper, due to the following reasons: *i*) at present time, it is unclear at which extent 5G devices operating at 26 [GHz] will be installed over the territory, and *ii*) there are not commercial gNBs operating at 26 [GHz] currently installed in Italy.

16. Clearly, the introduction of different types of gNBs operating on different frequencies greatly complicates the considered problem, mainly because the number of candidate locations is increased w.r.t. a scenario composed of homogeneous gNBs operating at the same frequency.

pixels \mathcal{P} . More in detail, we assume a pixel tessellation over the TMC area, with a pixel granularity equal to 10×10 [m²]. The total number of pixels $|\mathcal{P}|$ is then equal to 24318. Focusing then on the sensitive places, Fig. 6 highlights in yellow the areas hosting public parks, schools and/or churches. By adopting $R6$ regulation from Tab. 3, the installation of gNBs is prohibited within a minimum distance of $D^{\text{MIN}} = 100$ [m] from the external perimeter of these sensitive places.

We then analyze the setting of the remaining frequency-dependent parameters that are required as input. To this aim, Tab. 4 reports: *i*) $I_{(l,f)}^{\text{FREQ}}$ parameter (obtained from Fig. 5 by assuming $N^{\text{MAX}} = 1$), *ii*) distance-based parameters, *iii*) 5G EMF parameters, *iv*) 5G performance parameters, and *v*) 5G costs parameters. We now focus on the setting of the key parameters, while we refer the reader to the references reported in Tab. 4 for more information about the setting of each single parameter. More in depth, we assume that the maximum power $O_{(l,f)}^{\text{MAX}}$ that is radiated by a gNB operating over f_1 is actually higher than the one radiated by a gNB operating over f_2 . Although this setting may appear quite counter-intuitive at a first glance, since a micro gNB is expected to radiate less power than a macro gNB, we remind that $O_{(l,f)}^{\text{MAX}}$ refers to the maximum power, which can clearly differ w.r.t. the actual one that is received over the territory. When considering micro gNBs, $O_{(l,f)}^{\text{MAX}}$ is split across the radiating elements, and thus the actual power that is received over the territory is clearly lower compared to the maximum one. This effect is taken into account when setting the statistical scaling factor $R_{(l,f)}^{\text{STAT}}$. More in detail, we assume a strong statistical scaling factor that is applied to micro gNBs operating on f_1 , while no statistical scaling factor is applied to macro gNBs operating on f_2 . This choice is also motivated by the different goals of two gNB types, i.e., maximizing throughput for f_1 (and hence large spatial power variability) vs. ensuring coverage for f_2 (and hence less spatial power variability). Focusing then on the exclusion zones, we assume again two distinct values for f_1 and f_2 , which are set in accordance to the minimum distance guaranteeing a EMF level below the limit

TABLE 4
Setting of the frequency-related parameters.

	Parameter	$f1 = 3.7$ [GHz]	$f2 = 700$ [MHz]
	$I_{(l,f)}^{\text{FREQ}}$	Based on TMC scenario with $N^{\text{MAX}} = 1$.	
Distance	gNB height	10 [m] (Pole mounted)	25 [m] (Roof-top mounted)
	Pixel height	1.5 [m] (std. evaluation height)	
	$D_{(p,l,f)}$	Based on TMC scenario and gNB/pixel heights.	
5G EMF	$O_{(l,f)}^{\text{MAX}}$	200 [W] $\forall l \in \mathcal{L}$ [34]	65 [W] $\forall l \in \mathcal{L}$ (assumed to be in line with pre-5G technologies [14])
	η_f^{GAIN}	15 [dB] [14]	
	η_f^{LOSS}	2.32 [dB] [14]	
	$R_{(l,f)}^{\text{STAT}}$	0.25 $\forall l \in \mathcal{L}$ [27]	1 $\forall l \in \mathcal{L}$ (max. value)
	$R_{(l,f)}^{\text{TIME}}$	0.3 $\forall l \in \mathcal{L}$ [28]	
	Excl. Distance	11 [m] [35]	5 [m] (Roof excl. zone)
	$I_{(p,l,f)}^{\text{ZONE}}$	Based on the TMC scenario and the exclusion distances.	
	$P_{(p,f)}^{\text{BASE}}$	Based on real EMF measurements in TMC scenario.	
	$P_{(p,l,f)}^{\text{ADD}}$	Based on point source model [14] over TMC scenario and EMF parameters.	
	L_f	6 [V/m] ($R6$ of Tab. 3)	
5G Performance	D_f^{MAX}	200 [m] [36]	900 [m] [6], [22]
	γ_f	3.19 [37]	3 [37]
	σ_f^{SHAD}	8.2 [dB] [37]	6.8 [dB] [37]
	$z_{(l,p,j,f)}$	Log normal random variable [13].	
	$\beta_{(l,p,j,f)}$	Marzetta model [13] based on TMC scenario, γ_f and $z_{(l,p,j,f)}$.	
	N_f^{OFDM}	14 [38]	
	$N_f^{\text{OFDM-PILOT}}$	3 [13]	
	$\tau_f^{\text{COHERENCE}}$	500 [μs] [13]	
	δ_f	2.3 [μs] [38], [39]	4.7 [μs] [38], [39]
	Δ_f	30 [kHz] [38]	15 [kHz] [38]
	B_f	80 [MHz] [33]	20 [MHz] [33]
	$\epsilon_f^{\text{F-REUSE}}$	1 (unity frequency reuse)	
	S_f^{MIN}	Set to ensure 30 [Mbps] of min. throughput.	-
	Costs	$C_{(l,f)}^{\text{SITE}}$	14852 [€] $\forall l \in \mathcal{L}$ [36]
C_f^{EQUIP}		2791 [€] [36]	45673 [€] [36]
$\alpha_{(l,f)}$		$[10^1 - 10^7]$ [€] $\forall l \in \mathcal{L}$	$[10^1 - 10^4]$ [€] $\forall l \in \mathcal{L}$

of 6 [V/m] for a single gNB.¹⁷ Eventually, $P_{(p,f)}^{\text{BASE}}$ is retrieved from real measurements over the real scenario, with the methodology described in Appendix F.

Focusing then on the 5G performance parameters, the maximum coverage distance D_f^{MAX} is set to 200 [m] and to 900 [m] for $f1$ and $f2$, respectively (in accordance with [6], [22], [36]). More in depth, the setting of D_f^{MAX} can be based on e.g., minimum signal strength and/or prediction of radio resource availability and/or average load per gNB, depending on the operator's needs. Eventually, the path loss exponent γ_f is tuned in accordance with [37]. Clearly, this parameter can be easily varied to match different propagation conditions, e.g., urban, suburban, indoor, etc. Moreover,

17. The EMF is also computed in this case by applying the point source model of [14].

we assume that the minimum SIR is set in order to ensure a minimum pixel throughput of 30 [Mbps] for $f1$. In addition, we do not constrain the SIR over $f2$, since the goal of gNBs operating over this frequency is mainly to provide coverage. Therefore, even low throughput values may be admitted for $f2$.¹⁸ Although these throughput settings may appear relatively loose at a first glance, we will show that the actual throughput levels experienced over the served pixels are not negligible and in line with the 5G service requirements [21].

In the following step, we concentrate on the setting of the $\alpha_{(l,f)}$ parameters. We remind that such parameters are provided by the operator as input to our framework. However, since a precise estimation of $\alpha_{(l,f)}$ is beyond our goals, in this work we have performed a sensitivity analysis over huge ranges of $\alpha_{(l,f)}$, in order to consider the following cases: *i*) total costs dominate over coverage revenues, *ii*) revenues and costs are balanced, and *iii*) revenues are much higher than the costs. In this way, we are able to investigate the impact of $\alpha_{(l,f)}$ on the obtained planning on one side, and to provide an indications about the settings that ensure good coverage levels. For the sake of simplicity, we impose the same weights applied for all the candidate gNBs working at the same frequency.¹⁹ Moreover, we impose a wider interval of $\alpha_{(l,f1)}$ values w.r.t. $\alpha_{(l,f2)}$ because in this way we test the case in which serving a pixel with a micro gNB has a huge gain w.r.t. to a coverage provided by a macro gNB.

Finally, we provide the setting for the remaining parameters, namely Z_0 and N^{SER} . In particular, we set $Z_0 = 377$ [Ohm] (in accordance to [14]). In addition, we impose $N^{\text{SER}} = 2$. In this way, we consider a conservative case in which each pixel is served by at most two gNBs.²⁰

7 RESULTS

We code PLATEA algorithm in MATLAB R2019b and we run it on a Dell PowerEdge R230 equipped with Intel Xeon E3-1230 v6 3.5 [GHz] processors and 64 [GB] of RAM. We then describe the following steps: *i*) introduction of two reference algorithms as terms of comparison, *ii*) definition of evaluation metrics, *iii*) tuning of PLATEA parameters, *iv*) comparison of PLATEA vs. the reference algorithms, *v*) impact of planning parameters, *vi*) impact of pre-5G exposure levels, and *vii*) impact of frequency reuse scheme.

Reference Algorithms. Since the considered scenario is composed of thousands of pixels and dozens of candidate sites, it is not possible to solve the OPTPLAN-5G problem, which we remind belongs to the NP-Hard class. In order to introduce a term of comparison, we have implemented a simple algorithm based on an exhaustive search over all the possible micro and macro gNB combinations. We refer the interested reader to Appendix G for more details. In brief, the brute-force solution is not practically feasible, mainly due to very large computational times (much higher

18. We remind that, in any case, pixels beyond the maximum distance coverage D_f^{MAX} from a given gNB can not be served by the gNB.

19. In more complex scenarios, the values of $\alpha_{(l,f)}$ may be tuned for each location l , in order to prioritize locations that require huge amount of traffic (e.g., shopping malls, train stations, or airports) w.r.t. other ones. The evaluation of this aspect is left for future work.

20. The evaluation of N^{SER} values greater than 2 is left for future work.

TABLE 5
Breakdown of the evaluation metrics.

Metric	Notation/Expression	Reference Equations
Total Installation Costs	C^{TOT}	Eq. (32) (total costs computation).
Number of Installations	$N_{f1} = \sum_{l \in \mathcal{L}} y_{(l,f1)}, \quad N_{f2} = \sum_{l \in \mathcal{L}} y_{(l,f2)}$	-
Served Pixels	$X_{f1}^{\text{SERVED}} = \sum_{p \in \mathcal{P}} \sum_{l \in \mathcal{L}} x_{(p,l,f1)}, \quad X_{f2}^{\text{SERVED}} = \sum_{p \in \mathcal{P}} \sum_{l \in \mathcal{L}} x_{(p,l,f2)}$	-
Unserved pixels [%]	$X^{\text{NOT-SERVED}} = 100 \cdot \frac{\sum_{p \in \mathcal{P}: \{\sum_{l \in \mathcal{L}} \sum_{f \in \mathcal{F}} x_{(p,l,f)} = 0\}} (1 - \sum_{l \in \mathcal{L}} \sum_{f \in \mathcal{F}} x_{(p,l,f)})}{ \mathcal{P} }$	-
Pixel Throughput	$T_{(p,f)} = \sum_{l \in \mathcal{L}} \frac{B_f \Gamma_f}{\epsilon_f^{\text{REUSE}}} \log_2 (1 + S_{(p,l,f)}) \cdot x_{(p,l,f)}, \quad T_p = \sum_{f \in \mathcal{F}} T_{(p,f)}$	Eq. (14) (SIR computation on left hand side), Eq. (4) (Γ_f computation), Eq. (3) (throughput computation).
Average Pixel Throughput	$T_f^{\text{AVG}} = \frac{\sum_{p \in \mathcal{P}} T_{(p,f)}}{X_f^{\text{SERVED}}}, \quad T^{\text{AVG}} = \frac{\sum_{p \in \mathcal{P}} T_p}{ \mathcal{P} \cdot (1 - X^{\text{NOT-SERVED}}/100)}$	See computation of $T_p, T_{(p,f)}$ and $X^{\text{NOT-SERVED}}$.
Pixel EMF	$E_p = \sqrt{\sum_{f \in \mathcal{F}} \left[P_{(p,f)}^{\text{BASE}} \cdot (1 - w_p) + P_{(p,f)}^{\text{ADD-TS}} \right] \cdot Z_0}$	Eq. (27) (total power density computation in the numerator on left-hand side), Eq. (8) (electric field computation).
Average Pixel EMF	$E^{\text{AVG}} = \sqrt{\frac{\sum_{p \in \mathcal{P}^{\text{RES}}} \sum_{f \in \mathcal{F}} \left[P_{(p,f)}^{\text{BASE}} \cdot (1 - w_p) + P_{(p,f)}^{\text{ADD-TS}} \right]}{ \mathcal{P}^{\text{RES}} }} \cdot Z_0$	See computation of E_p .

than the relatively loose time constraints that may be allowed for solving planning problems). To overcome such issue, we have designed two sub-optimal (yet meaningful) algorithms in order to better position PLATEA. The two solutions, named EVALUATION ALGORITHM (EA) and MAXIMUM COVERAGE MACRO ALGORITHM (MCMA) are detailed in Appendix H. In brief, EA and MCMA evaluate the feasibility constraints of a random set of installed gNBs, without exploring the possible site combinations (which are instead analyzed by PLATEA). In this way, we are able to compare PLATEA against two low-complexity solutions. More in depth, EA explores a single possible deployment (which is generated from a fixed number of gNBs, passed as input to the algorithm). On the other hand, MCMA goes one step further, by selecting the set of macro gNBs operating on $f2$ maximizing the service coverage, given an integer number of $f1$ gNBs that have to be installed over the territory.

Evaluation Metrics. We then formally introduce the metrics to evaluate the performance of PLATEA, EA and MCMA. To this aim, Tab. 5 reports: *i*) total installation costs C^{TOT} , *ii*) number N_{f1} (N_{f2}) of $f1$ ($f2$) gNBs installations, *iii*) number of pixels X_{f1}^{SERVED} (X_{f2}^{SERVED}) served by $f1$ ($f2$) gNBs, *iv*) percentage of unserved pixels $X^{\text{NOT-SERVED}}$, *v*) per-frequency $T_{(p,f)}$ and total T_p pixel throughput, *vi*) average pixel throughput over each frequency T_f^{AVG} and over all frequencies T^{AVG} , both of them computed over the pixels that are served by gNBs, *vii*) pixel EMF E_p , *viii*) average pixel EMF E^{AVG} , computed over the whole set of pixels in the scenario. For each metric, the table reports the metric name, the mathematical notation, and the reference equation(s) used to compute the metric.

Tuning of PLATEA Parameters. We initially concentrate on the impact of the $\alpha_{(l,f)}$ terms that control the behavior of the objective function in PLATEA. As already mentioned Sec. 6, we explore a wide range of values for both $\alpha_{(l,f1)}$ and $\alpha_{(l,f2)}$, in order to test different conditions, e.g., costs minimization, balance between costs and revenues, revenues maximization. In addition, we initially assume the dismissal of legacy pre-5G Base Stations that

radiate over TMC, in order to evaluate the performance of PLATEA in a clean-slate condition. Therefore, we set $P_{(p,f)}^{\text{BASE}} = 0 \quad \forall f \in \mathcal{F}, p \in \mathcal{P}$. We then run PLATEA over the selected ranges of $\alpha_{(l,f1)}$ and $\alpha_{(l,f2)}$, by picking values on logarithmic scales. Fig. 7 highlights the obtained results in terms of: *i*) total installation costs C^{TOT} (Fig. 7(a)), *ii*) number N_{f1} of $f1$ gNBs (Fig. 7(b)), *iii*) number N_{f2} of $f2$ gNBs (Fig. 7(c)), *iv*) percentage of not served pixels $X^{\text{NOT-SERVED}}$ (Fig. 7(d)), *v*) average pixel throughput T^{AVG} (Fig 7(e)) and *vi*) average electric field E^{AVG} (Fig. 7(f)).

Several considerations hold by analyzing in detail Fig. 7. First, C^{TOT} is proportional to $\alpha_{(l,f1)}$ and $\alpha_{(l,f2)}$ (Fig. 7(a)), due to the fact that the weights play a major role in determining the objective function, e.g., cost minimization, service maximization or a mixture between them. Clearly, $\alpha_{(l,f1)}$ ($\alpha_{(l,f2)}$) only affects N_{f1} (N_{f2}), as shown in Fig. 7(b) (Fig. 7(c)). In addition, $X^{\text{NOT-SERVED}}$ is inversely proportional to $\alpha_{(l,f2)}$ (Fig. 7(d)). For example, when $\alpha_{(l,f2)} \approx 10$, more than 10% of pixels are not served by any gNB. This is due to the fact that the number of $f2$ gNBs that are installed passes from 3 to 1 (see Fig. 7(c)), thus creating coverage holes. On the other hand, the variation of $\alpha_{(l,f1)}$ has a clear impact on $X^{\text{NOT-SERVED}}$ only when $\alpha_{(l,f2)} \approx 10$, i.e., when $f2$ gNBs are not able to cover the whole territory. Moreover, Fig 7(e) reveals that T^{AVG} has a complex trend, which results from the combination of: *i*) the coverage provided by $f1$ and $f2$ gNBs installed over the territory, *ii*) the amount of interference, which tends to be impacted by the number of neighboring gNBs operating at the same frequency, and *iii*) the percentage of served pixels, since T^{AVG} is computed over the pixels that receive service coverage from at least one gNB. As a consequence, T^{AVG} is not always proportional or inversely proportional with $\alpha_{(l,f)}$. For example, the maximum value of T^{AVG} is achieved when $\alpha_{(l,f2)} = 10$, which however leads to a huge number of unserved pixels (i.e., more than 10%). Finally, E^{AVG} is proportional to $\alpha_{(l,f)}$, due to the variation in the number of radiating sources that contribute to the EMF exposure. However, we point out that the average EMF level is almost one order of magnitude lower than the 6 [V/m] restrictive limit.

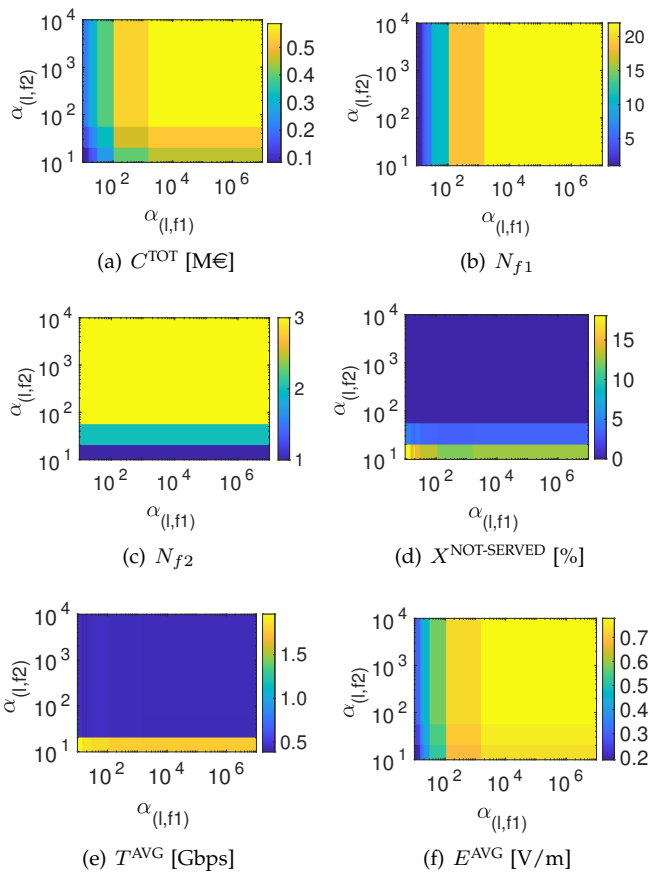
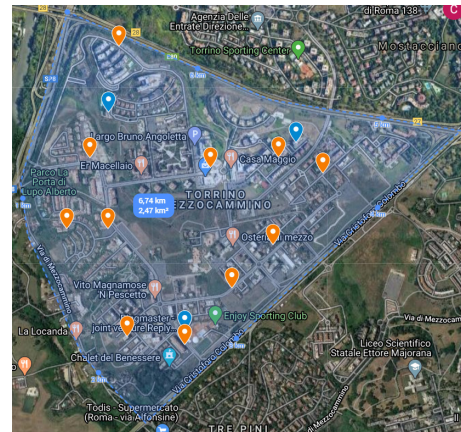


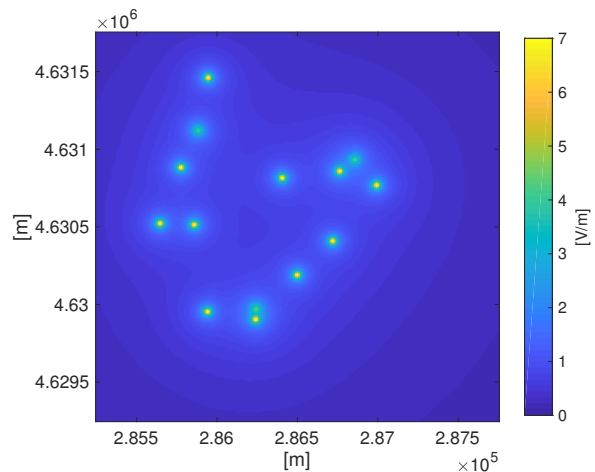
Fig. 7. Impact of $\alpha_{(l,f)}$ variation on: *i*) total installation costs C^{TOT} , *ii*) number N_{f1} of $f1$ gNBs, *iii*) number N_{f2} of $f2$ gNBs, *iv*) percentage of not served pixels $X^{\text{NOT-SERVED}}$, *v*) average pixel throughput T^{AVG} , *vi*) average electric field E^{AVG} .

Based on the above considerations, we select $\alpha_{(l,f1)} = 50$ [€] and $\alpha_{(l,f2)} = 500$ [€] henceforth. In this way, we balance between: *i*) increasing T^{AVG} , *ii*) reducing C^{TOT} , *iii*) minimizing $X^{\text{NOT-SERVED}}$, *iv*) reducing E^{AVG} . To give more insights, Fig. 8 shows a run of the planning selected by PLATEA with the aforementioned setting. Interestingly, only a subset of the candidate gNBs, i.e., 11 $f1$ gNBs and 3 $f2$ gNBs, are deployed over the TMC scenario (Fig. 8(a)). On the other hand, the resulting EMF levels are always pretty low (see Fig. 8(b)), with an electric field close to the 6 [V/m] limit only in proximity to the $f1$ gNBs.

Algorithms Comparison. In the following, we compare the performance of PLATEA against EA and MCMA. Unless otherwise specified, we compute each metric by averaging the results over 10 independent runs. Focusing on the number of $f1$ and $f2$ gNBs selected by PLATEA, we have found that our solution requires on average $N_{f1} = 10.7$ and $N_{f2} = 3$, respectively. Consequently, we have passed to EA and MCMA a number of $f1$ gNBs equal to 11. In addition, EA requires the number of $f2$ gNB, which is set to 3. Tab. 6 reports the performance of the algorithms over the different metrics. More in detail, the total installation costs C^{TOT} of PLATEA and EA are clearly lower than the ones of MCMA. Clearly, since EA requires as input the same (integer) number of $f1$ and $f2$ gNBs of PLATEA, it is natural that the two solutions achieve almost the same C^{TOT} . On the other hand, MCMA requires a larger number of $f2$ gNBs, in order



(a) Map of installed gNBs (orange pins: $f1$ gNBs, blue pins: $f2$ gNBs)



(b) Electric field levels E_p [V/m]

Fig. 8. Visualization of the best scenario retrieved by PLATEA with $\alpha_{(l,f1)} = 50$ [€] and $\alpha_{(l,f2)} = 500$ [€].

to ensure full coverage. Focusing then on the number of pixels served by $f1$ and $f2$ gNBs, PLATEA operates a wiser choice compared to EA and MCMA, with several pixels that are served by $f1$ gNBs. Clearly, MCMA guarantees full coverage of the territory, $X^{\text{NOT-SERVED}} = 0\%$. On the other hand, 6% of pixels are not served with EA. Eventually, PLATEA ensures service coverage for 99.97% of pixels. Moreover, PLATEA achieves a clearly higher throughput T^{AVG} compared to EA and MCMA. In particular, the throughput difference of PLATEA w.r.t. EA and MCMA is huge, i.e., more than 90 [Mbps] on average. In addition, we can note that T_f^{AVG} obtained by PLATEA is consistently higher than EA and MCMA over both frequencies. Finally, the EMF levels introduced by PLATEA and EA are clearly lower than MCMA. In conclusion, PLATEA outperforms both MCMA and EA when the different metrics are jointly considered. We refer the interested reader to Appendix I for further comparisons between PLATEA and the reference algorithms. In the following, we will analyze in more detail the impact of the planning parameters on the PLATEA performance.

Impact of planning parameters. We then focus on the impact of the planning parameters, namely: *i*) the scaling

TABLE 6

Comparison of PLATEA vs. reference algorithms EA and MCMA.

Metric	EA	MCMA	PLATEA
C^{TOT} [k€]	391.4	<u>555.8</u>	386.1
N_{f1}	11	11	10.7
N_{f2}	3	<u>5.5</u>	3
X_{f1}^{SERVED}	<u>7960</u>	<u>7960</u>	<u>9103</u>
X_{f2}^{SERVED}	<u>14897</u>	<u>16357</u>	<u>15307</u>
$X^{\text{NOT-SERVED}}$ [%]	<u>6</u>	0	<u>0.03</u>
T^{AVG} [Mbps]	<u>337.1</u>	<u>319.3</u>	<u>428.3</u>
T_{f1}^{AVG} [Mbps]	<u>356.6</u>	<u>356.6</u>	<u>391.5</u>
T_{f2}^{AVG} [Mbps]	<u>199.3</u>	<u>166.4</u>	<u>245.2</u>
E^{AVG} [V/m]	0.57	<u>0.63</u>	0.57

parameters $R_{(l,f)}^{\text{TIME}}$ and $R_{(l,f)}^{\text{STAT}}$, which affect the EIRP and consequently the EMF exposure generated by gNBs and *ii*) the minimum distance from sensitive places D^{MIN} , which influences the subset of sites that can host gNBs. Focusing on *i*) we perform a sensitivity analysis by running PLATEA over a wide range of $R_{(l,f)}^{\text{TIME}}$ and $R_{(l,f)}^{\text{STAT}}$ values. For the sake of simplicity, we impose $R_{(l,f)}^{\text{TIME}} \in [0.1 - 0.6] \quad \forall f \in \mathcal{F}, l \in \mathcal{L}$. On the other hand, we set $R_{(l,f1)}^{\text{TIME}} \in [0.1 - 0.6] \quad \forall l \in \mathcal{L}$ and $R_{(l,f2)}^{\text{STAT}} = 1 \quad \forall l \in \mathcal{L}$. In this way, $f1$ gNBs are subject to temporal and statistical scaling factors, while $f2$ gNB are affected only by temporal scaling factors.

Fig. 9 reports the obtained results in terms of: *i*) average EMF E^{AVG} , *ii*) number N_{f1} of $f1$ gNBs, *iii*) number N_{f2} of $f2$ gNBs, *iv*) average throughput T^{AVG} , *v*) percentage of not served pixels $X^{\text{NOT-SERVED}}$, *vi*) number of pixels served by $f2$ gNBs X_{f2}^{SERVED} . Interestingly, the choice of $R_{(l,f)}^{\text{TIME}}$ and $R_{(l,f)}^{\text{STAT}}$ has a huge impact on the obtained planning. In particular, when $R_{(l,f)}^{\text{TIME}}$ and $R_{(l,f)}^{\text{STAT}}$ are close to 0.1, the average EMF exposure is very low (i.e., lower than 0.4 [V/m]), as shown at the bottom left corner of Fig. 9(a). In this region, PLATEA installs more than 10 $f1$ gNB (Fig. 9(b)) and 3 $f2$ gNBs (Fig. 9(c)). In addition, a large throughput is achieved (Fig. 9(d)) and (almost) all the pixels are served (Fig. 9(e)). On the other hand, when $R_{(l,f)}^{\text{TIME}}$ and $R_{(l,f)}^{\text{STAT}}$ are increased, the average EMF tends to increase and therefore it is challenging to ensure the strict EMF constraints in the proximity of the installed gNBs. Therefore, the number of installed gNBs is reduced, the throughput is decreased and the percentage of not served pixels abruptly increases. Eventually, for large values of $R_{(l,f)}^{\text{TIME}}$ and $R_{(l,f)}^{\text{STAT}}$ (top right corner of subfigures), it is not possible to install any gNB and therefore all the pixels are unserved. In addition, we can note that a frontier region emerges for intermediate values of the scaling parameters. Interestingly, for most of $R_{(l,f)}^{\text{TIME}}$ and $R_{(l,f)}^{\text{STAT}}$ combinations laying on the frontier, a huge amount of pixels is served by $f2$ gNBs (Fig. 9(f)).

Summarizing, our results demonstrate that the setting of the scaling parameters plays a major role in the planning of 5G networks, especially for countries adopting strict EMF limits. As a side comment, we believe that the methodology to estimate the values of $R_{(l,f)}^{\text{TIME}}$ and $R_{(l,f)}^{\text{STAT}}$ should be integrated in the national EMF regulations. Clearly, the exact settings of the scaling parameters depend on the considered scenario.

We then evaluate the impact of varying D^{MIN} , which we

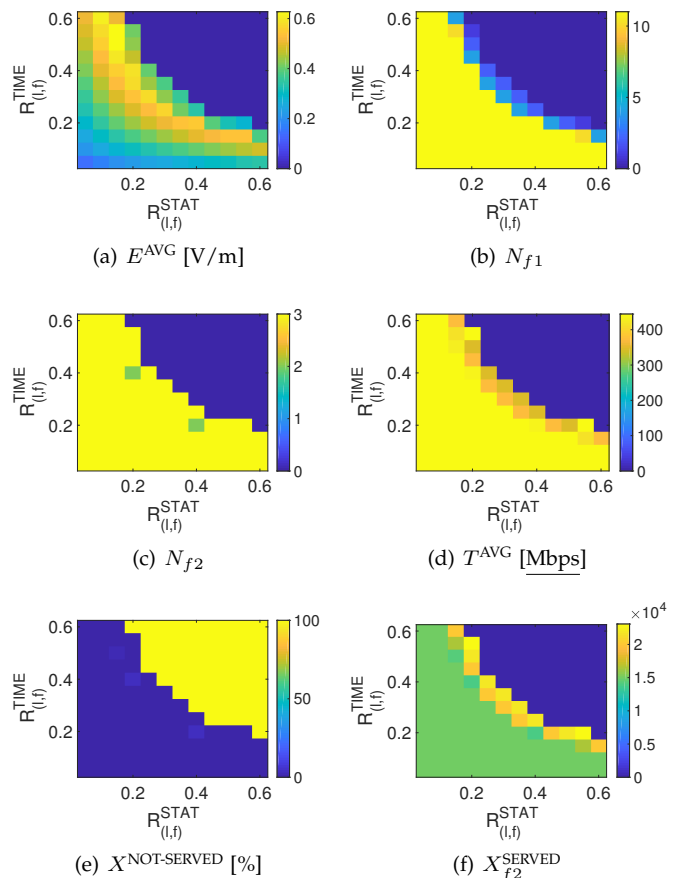


Fig. 9. Impact of the variation of the scaling parameters on: *i*) average electric field E^{AVG} , *ii*) number N_{f1} of $f1$ gNBs, *iii*) number N_{f2} of $f2$ gNBs, *iv*) average throughput T^{AVG} , *v*) percentage of not served pixels $X^{\text{NOT-SERVED}}$, *vi*) number of pixels served by $f2$ gNBs X_{f2}^{SERVED} .

remind is an additional restriction imposed by the municipality of Rome. We report here the main outcomes from this test, while we refer the interested reader to Appendix I.3 for more details. In brief, values of $D^{\text{MIN}} < 100$ [m] do not significantly alter the results presented so far. On the contrary, a value of $D^{\text{MIN}} = 150$ [m] introduces huge limitations on the gNBs installations, and consequently on the 5G service in terms of throughput and number of served pixels.

Impact of pre-5G exposure levels. We then focus on the impact of adding the pre-5G exposure term on the 5G planning. Due to the lack of space, we refer the reader to Appendix I.4 for a detailed report about these outcomes, while here we briefly summarize the salient features. In brief, when the pre-5G exposure is increased, we can note: *i*) a reduction in the number of $f1$ gNBs, and consequently of total costs, *ii*) an increase in the number of pixels served by $f2$ gNBs, *iii*) a slight throughput decrease, and *iv*) an EMF increase, mainly due to the pre-5G exposure term. Overall, these results prove that the performance metrics are impacted by the level of background exposure. However, PLATEA is always able to retrieve a feasible planning, with a percentage of unserved pixels at most equal to 0.16%.

Impact of frequency reuse scheme. In the last part of our work, we have investigated the impact of changing

the frequency reuse factor $\epsilon_f^{\text{F-REUSE}}$. We refer the reader to Appendix I.5 for the details. In brief, we have found that, as $\epsilon_f^{\text{F-REUSE}}$ is increased, the throughput, the total costs and the average EMF levels are decreased, mainly because less gNBs operating on frequency f_1 are installed.

8 CONCLUSIONS AND FUTURE WORKS

We have focused on the problem of planning a 5G network under service and EMF constraints. To this aim, we have targeted an objective function that balances between gNB installation costs and 5G service coverage level. After providing the OPTPLAN-5G MILP formulation, we have demonstrated that the considered problem is NP-Hard, and therefore very challenging to be solved even for small problem instances. To face this issue, we have designed the PLATEA algorithm, which is able to select a 5G planning by iterating over the set of candidate gNBs. In addition, PLATEA exploits the linear constraints that have been defined for OPTPLAN-5G. We have then considered the TMC scenario, which is subject to very strict EMF regulations that include minimum distances from sensitive places and very stringent EMF limits.

Results, obtained by running PLATEA over the considered scenario, prove that our solution outperforms EA and MCMA. In addition, we have demonstrated that the 5G planning is overall feasible, i.e., it is possible to serve a huge amount of pixels while limiting the installation costs and while ensuring the EMF constraints outside the exclusion zones of the installed gNBs. However, our work points out an important aspect: the scaling parameters that are used to estimate the exposure level from 5G gNBs play a fundamental role in determining the problem feasibility and consequently the set of installed gNBs. Eventually, when pre-5G exposure is considered, PLATEA is still able to retrieve an admissible planning, with a moderate impact on pixel throughput. Finally, the adopted frequency reuse scheme strongly influences the obtained planning.

We believe that this work could be the first step towards a more comprehensive approach. First of all, the integration of gNBs operating on mm-Waves may be an interesting future work. In addition, the optimization of the scaling parameters may be another research avenue. Eventually, we plan to integrate detailed propagation models (e.g., including indoor evaluation), more complex EMF models, more detailed service models (even different than a Massive-MIMO system), fronthaul/backhaul constraints governing the installation of gNBs, multiple spectrum sharing options, multiple power budget levels across the gNBs operating at the same frequency, as well as the integration of edge/caching considerations in the adopted models. Finally, we will investigate possible algorithmic solutions to parallelize the planning computation when large territory areas are taken under consideration.

REFERENCES

- [1] L. Chiaraviglio, A. S. Cacciapuoti, G. Di Martino, M. Fiore, M. Montesano, D. Trucchi, and N. Blefari-Melazzi, "Planning 5g networks under emf constraints: State of the art and vision," *IEEE Access*, vol. 6, pp. 51021–51037, 2018.
- [2] E. J. Oughton, K. Katsaros, F. Entezami, D. Kaleshi, and J. Crowcroft, "An open-source techno-economic assessment framework for 5G deployment," *IEEE Access*, vol. 7, pp. 155930–155940, 2019.
- [3] E. Amaldi, A. Capone, and F. Malucelli, "Planning umts base station location: Optimization models with power control and algorithms," *IEEE Transactions on Wireless Communications*, vol. 2, no. 5, pp. 939–952, 2003.
- [4] A. R. Mishra, *Fundamentals of cellular network planning and optimization: 2G/2.5 G/3G... evolution to 4G*. John Wiley & Sons, 2004.
- [5] L. Chiaraviglio, A. Elzanaty, and M.-S. Alouini, "Health risks associated with 5g exposure: A view from the communications engineering perspective," *arXiv preprint arXiv:2006.00944*, 2020.
- [6] L. Chiaraviglio, J. Galán-Jiménez, M. Fiore, and N. Blefari-Melazzi, "Not in my neighborhood: A user equipment perspective of cellular planning under restrictive emf limits," *IEEE Access*, vol. 7, pp. 6161–6185, 2018.
- [7] H. M. Madjar, "Human radio frequency exposure limits: An update of reference levels in europe, usa, canada, china, japan and korea," in *2016 International Symposium on Electromagnetic Compatibility-EMC EUROPE*, pp. 467–473, IEEE, 2016.
- [8] International Commission on Non-Ionizing Radiation Protection (ICNIRP), "ICNIRP guidelines on limiting exposure to time-varying electric, magnetic and electromagnetic fields (100 kHz to 300 GHz)." Available at: <https://www.icnirp.org/cms/upload/publications/ICNIRPrfgdl2020.pdf>, Jul. 2020. Last Accessed: 25th May 2020.
- [9] "Office of engineering technology (OET) bulletin 65," Tech. Rep. Ed. 97-01, Federal Communications Commission (FCC), Aug. 1997.
- [10] ITU-T K Supplement 14: *The impact of RF-EMF exposure limits stricter than the ICNIRP or IEEE guidelines on 4G and 5G mobile network deployment*. Available at <https://www.itu.int/rec/T-REC-K.Sup14-201909-I>, Last Accessed on 6th Apr. 2020.
- [11] *Legge quadro 22/02/2001, n. 36 (G.U. 08/03/2001, n. 55) "Legge quadro sulla protezione dalle esposizioni a campi elettrici, magnetici ed elettromagnetici"*. Available at: <https://www.normattiva.it/uri-res/N2Ls?urn:nir:stato:legge:2001-02-22;36?vig=,> Last Accessed on 27th July 2020.
- [12] *Regolamento per la Localizzazione, L'installazione e la Modifica Degli Impianti di Telefonia Mobile, ai Sensi Dell'art. 8, Comma 6, Della Legge n. 36 Del 22 Febbraio 2001 e per la Redazione del Piano, ex Art. 105, Comma 4 Delle NTA del PRG Vigente, Nonche per L'adozione di un Sistema di Monitoraggio Delle Sorgenti di Campo Elettrico, Magnetico ed Elettromagnetico*. Available at: https://www.comune.roma.it/web-resources/cms/documents/DACDelib_N_26_14.05.2015.pdf, Last Accessed on 27th July 2020.
- [13] T. L. Marzetta, "Noncooperative cellular wireless with unlimited numbers of base station antennas," *IEEE Transactions on Wireless Communications*, vol. 9, no. 11, pp. 3590–3600, 2010.
- [14] ITU-T K.70: *Mitigation techniques to limit human exposure to EMFs in the vicinity of radiocommunication stations*. Available at <https://www.itu.int/rec/T-REC-K.70-201801-I/en>, Last Accessed on 26th Feb. 2020.
- [15] M. Matalatala, M. Deruyck, E. Tanghe, S. Goudos, L. Martens, and W. Joseph, "Joint optimization towards power consumption and electromagnetic exposure for massive MIMO 5G networks," in *Proc. 29th Annual International Symposium on Personal, Indoor and Mobile Radio Communications (IEEE PIMRC), Bologna, Italy*, pp. 1208–1214, Sep. 2018.
- [16] M. Matalatala, M. Deruyck, S. Shikhantsov, E. Tanghe, D. Plets, S. Goudos, K. E. Psannis, L. Martens, and W. Joseph, "Multi-objective optimization of massive MIMO 5G wireless networks towards power consumption, uplink and downlink exposure," *Applied Sciences*, vol. 9, no. 22, 2019.
- [17] J. Pérez-Romero, O. Sallent, R. Ferrús, and R. Agustí, "Knowledge-based 5g radio access network planning and optimization," in *2016 International Symposium on Wireless Communication Systems (ISWCS)*, pp. 359–365, IEEE, 2016.
- [18] A. Taufique, M. Jaber, A. Imran, Z. Dawy, and E. Yacoub, "Planning wireless cellular networks of future: Outlook, challenges and opportunities," *IEEE Access*, vol. 5, pp. 4821–4845, 2017.
- [19] N. Saxena, A. Roy, and H. Kim, "Efficient 5g small cell planning with embms for optimal demand response in smart grids," *IEEE Transactions on Industrial Informatics*, vol. 13, no. 3, pp. 1471–1481, 2017.

- [20] M. U. Khan, A. García-Armada, and J. Escudero-Garzás, "Service-based network dimensioning for 5g networks assisted by real data," *IEEE Access*, vol. 8, pp. 129193–129212, 2020.
- [21] *Service requirements for the 5G system (3GPP TS 22.261 version 16.2.0 Release 16)*. Available at <https://portal.3gpp.org/desktopmodules/Specifications/SpecificationDetails.aspx?specificationId=3107>, Last Accessed on 28th July 2020.
- [22] M. N. Patwary, S. J. Nawaz, M. A. Rahman, S. K. Sharma, M. M. Rashid, and S. J. Barnes, "The potential short-and long-term disruptions and transformative impacts of 5g and beyond wireless networks: Lessons learnt from the development of a 5g testbed environment," *IEEE Access*, vol. 8, pp. 11352–11379, 2020.
- [23] International Commission on Non-Ionizing Radiation Protection (ICNIRP), "Guidelines for limiting exposure to time-varying electric, magnetic, and electromagnetic fields (up to 300 GHz)," *Health Physics*, vol. 74, no. 4, pp. 494–522, 1998.
- [24] *TESTO COORDINATO DEL DECRETO-LEGGE 18 Ottobre 2012, n. 179 Ulteriori Misure Urgenti per la Crescita del Paese*. Available at: www.gazzettaufficiale.it/eli/id/2012/12/18/12A13277/sg, Last Accessed on 27th July 2020.
- [25] *IEC 62232:2017 Determination of RF field strength, power density and SAR in the vicinity of radiocommunication base stations for the purpose of evaluating human exposure*. Available at <https://webstore.iec.ch/publication/28673>, Last Accessed on 27th Feb. 2020.
- [26] *IEC TR 62669:2019 Case studies supporting IEC 62232 - Determination of RF field strength, power density and SAR in the vicinity of radiocommunication base stations for the purpose of evaluating human exposure*. Geneva, Apr. 2019. Available at <https://webstore.iec.ch/publication/62014>, Last Accessed on 27th Feb. 2020.
- [27] B. Thors, A. Furuskär, D. Colombi, and C. Törnevik, "Time-averaged realistic maximum power levels for the assessment of radio frequency exposure for 5G radio base stations using massive MIMO," *IEEE Access*, vol. 5, pp. 19711–19719, 2017.
- [28] *5G Is Landing: Are We Ready?* Available (In Italian) at https://www.arpae.it/cms3/documenti/_cerca_doc/ecoscienza/ecoscienza2019_4/Ecoscienza2019_4.pdf, Last Accessed on 26th Feb. 2020.
- [29] *Evaluation criteria for authorization requests of radio base stations with mMimo (in Italian)*. Available at: <https://www.snpambiente.it/wp-content/uploads/2019/10/Delibera-59-Criteri-valutazione-antenne-mMIMO.pdf>, Last Accessed on 27th July 2020.
- [30] A. Kamar, S. J. Nawaz, M. Patwary, M. Abdel-Maguid, et al., "Optimized algorithm for cellular network planning based on terrain and demand analysis," in *2nd IEEE International Conference on Computer Technology and Development, Cairo, Egypt*, pp. 359–364, 2010.
- [31] S. Martello, "Knapsack problems: algorithms and computer implementations," *Wiley-Interscience series in discrete mathematics and optimization*, 1990.
- [32] *PLATEA Source Code*. Available at <https://www.dropbox.com/sh/fdapa900pw3y46k/AABZ1eZkJoCdHP-G-xhNL9uha?dl=0>, Last Accessed on 30th November 2020.
- [33] *5G Frequency Auction in Italy (In Italian)*. Available at <https://www.mise.gov.it/index.php/it/comunicazioni/servizi-alle-impres/tecnologia-5g/bando-5g>, Last Accessed on 28th July 2020.
- [34] *Antenna Integrated Radio Unit Description - Ericsson*. Available at <http://www.1com.net/wp-content/uploads/2019/09/sales@1com.com-Ericsson-AIR-6488-Integrated-Radio-Unit-Datasheet.pdf>, Last Accessed on 28th July 2020.
- [35] *Impact of EMF limits on 5G network roll-out*. Available at https://www.itu.int/en/ITU-T/Workshops-and-Seminars/20171205/Documents/S3_Christer_Tornevik.pdf, Last Accessed on 25th Feb. 2020.
- [36] E. J. Oughton, Z. Frias, S. van der Gaast, and R. van der Berg, "Assessing the capacity, coverage and cost of 5g infrastructure strategies: Analysis of the netherlands," *Telematics and Informatics*, vol. 37, pp. 50–69, 2019.
- [37] S. Sun, T. S. Rappaport, T. A. Thomas, A. Ghosh, H. C. Nguyen, I. Z. Kovács, I. Rodriguez, O. Koymen, and A. Partyka, "Investigation of prediction accuracy, sensitivity, and parameter stability of large-scale propagation path loss models for 5g wireless communications," *IEEE Transactions on Vehicular Technology*, vol. 65, no. 5, pp. 2843–2860, 2016.
- [38] *5G NR Physical channels and modulation (3GPP TS 38.211 version 15.3.0 Release 15)*. Available at https://www.etsi.org/deliver/etsi-ts/138200_138299/138211/15.03.00_60/ts_138211v150300p.pdf, Last Accessed on 28th July 2020.
- [39] *5G/NR - Frame Structure*. Available at https://www.sharetechnote.com/html/5G/5G_FrameStructure.html, Last Accessed on 26th July 2020.



Luca Chiaraviglio (M'09-SM'16) is Associate Professor at the University of Rome Tor Vergata (Italy). He holds a Ph.D. in Telecommunication and Electronics Engineering, obtained from Politecnico di Torino (Italy). Luca has co-authored 140+ papers published in international journals, books and conferences. He is TPC member of IEEE INFOCOM, associate editor for IEEE COMMUNICATIONS MAGAZINE and IEEE TRANSACTIONS ON GREEN COMMUNICATIONS AND NETWORKING, and Specialty Chief Editor of FRONTIERS IN COMMUNICATIONS AND NETWORKS. Luca has received the Best Paper Award at IEEE VTC-Spring 2020, IEEE VTC-Spring 2016 and ICIN 2018, all of them appearing as first author. Some of his papers are listed as Best Readings on Green Communications by IEEE. Moreover, he has been recognized as an author in the top 1% most highly cited papers in the ICT field worldwide. His current research topics cover 5G networks, optimization applied to telecommunication networks, and health risks assessment of 5G communications.



Cristian Di Paolo graduated in ICT and Internet Engineering from the University of Rome Tor Vergata in February 2020. Between January and March 2020 he has been a CNIT Researcher. He currently works as Network Engineer at Huawei.



Nicola Blefari-Melazzi is currently a Full Professor of telecommunications with the University of Rome "Tor Vergata", Italy. He is currently the Director of CNIT, a consortium of 37 Italian Universities. He has participated in over 30 international projects, and has been the principal investigator of several EU funded projects. He has been an Evaluator for many research proposals and a Reviewer for numerous EU projects. He is the author/coauthor of about 200 articles, in international journals and conference proceedings.

His research interests include the performance evaluation, design and control of broadband integrated networks, wireless LANs, satellite networks, and of the Internet.

APPENDIX A

CONSIDERATIONS ON THE POINT SOURCE MODEL

Hereafter, we report some considerations about the point source model and its positioning against synthetic and full-wave models. In brief, the point source model is based on a conservative approach, which in general brings an over-estimation EMF w.r.t to the exposure level that is then experienced once the network is put under operation. As a result, the exposure levels that are observed after the gNB installation are generally lower than the ones predicted by the point source model during the planning phase. Clearly, if the adherence to the exposure limit is verified from the point source model, this condition will also hold after the installation of the deployment.

On the other hand, both synthetic and full-wave models are able to provide a better estimation of the EMF, which can be an appealing property from the operator's side. However, such approaches introduce different challenges, which include:

- an increased complexity in integrating these models in the considered framework;
- a strong dependence with extremely detailed antenna parameters, which are typically not disclosed by operators.

In conclusion, we have selected the point source model because in this way we adopt a conservative approach to verify the compliance of the EMF levels against the regulations. In addition, we exploit the model to generate a set of linear constraints that are easily integrated in our framework.

APPENDIX B

PIXEL TESSELLATION

By applying a tessellation based on pixels, three important goals can be met, namely:

- 1) the power density terms are computed over the whole area under consideration. More in depth, we evaluate the power density that is received over the pixel center from all the installed gNBs. In this way, we are able to extend the EMF compliance assessment over the whole territory. In addition, we model the presence of exclusion zones in proximity to the installed gNBs, i.e., zones of the territory that are not accessed by users and therefore in such zones the EMF compliance assessment is not required for the general public;
- 2) we evaluate the throughput/coverage in each pixel over the territory, and not only in the locations where the users are supposed to be. This assumption appears to be meaningful in the context of 5G, especially for the eMBB scenario [21]. In this way, it is possible to control the amount of throughput provided to each pixel, and consequently to the UE that are located in the pixel;
- 3) a minimum throughput requirement may be introduced for each pixel rather than for single users. In this way, it is possible to (indirectly) take into account the effects of UE densification and/or UE

mobility. For example, by assigning different values of required throughput, it is possible to model high density zones, where the throughput requirements are high, compared to other zones, which instead are not visited by users. In a similar way, it is possible to vary the throughput requirements based on the UE mobility, e.g., by increasing the throughput for the zones that are subject to high UE mobility, in order to take into account the effect of handovers and/or possible traffic spikes.

Clearly, our framework guarantees throughput requirements for each pixel, which is not exactly equivalent to guarantee the same throughput for any user within the pixel. Intuitively, in fact, the radio resources consumed by a given pixel have to be split among the users located in the pixel. To further complicate this picture, the allocation of radio resources over the same pixel may be not uniform across the users, due to different service/QoS requirements. Since the goal of the planing phase is not to consider this level of detail, in this work we are assuming throughput requirements on a pixel base, and not on single users. Clearly, the pixel throughput corresponds to the maximum value that can be experienced by a UE within the pixel.

APPENDIX C

NOTATION

Tab. 7 reports the main notation defined in the problem formulation.

APPENDIX D

SIR LINEARIZATION

In order to linearize Eq. (14), we initially exploit the following equivalence:

$$\sum_{l_2 \neq l \in \mathcal{L}} \beta_{(l,p,l_2,f)}^2 \cdot y_{(l_2,f)} = \sum_{l_2 \in \mathcal{L}} \beta_{(l,p,l_2,f)}^2 \cdot y_{(l_2,f)} - \beta_{(l,p,l,f)}^2 \cdot y_{(l,f)} \quad (38)$$

By assuming that the right-hand side of Eq. (38) is greater than or equal to 0, we replace the denominator of Eq. (14) with Eq. (38), thus obtaining:

$$\beta_{(l,p,l,f)}^2 \cdot y_{(l,f)} \geq S_f^{\text{MIN}} \cdot x_{(p,l,f)} \cdot \left[\sum_{l_2 \in \mathcal{L}} \beta_{(l,p,l_2,f)}^2 \cdot y_{(l_2,f)} - \beta_{(l,p,l,f)}^2 \cdot y_{(l,f)} \right], \quad \forall p \in \mathcal{P}, l \in \mathcal{L}, f \in \mathcal{F} \quad (39)$$

We then divide both sides of the constraint by the left hand side term, thus obtaining:

$$S_f^{\text{MIN}} \cdot x_{(p,l,f)} \cdot \left[\frac{\sum_{l_2 \in \mathcal{L}} \beta_{(l,p,l_2,f)}^2 \cdot y_{(l_2,f)}}{\beta_{(l,p,l,f)}^2 \cdot y_{(l,f)}} - 1 \right] \leq 1, \quad \forall p \in \mathcal{P}, l \in \mathcal{L}, f \in \mathcal{F} \quad (40)$$

The previous constraint is equivalent to the following one:

$$S_f^{\text{MIN}} \left[\frac{\sum_{l_2 \in \mathcal{L}} \beta_{(l,p,l_2,f)}^2 \cdot y_{(l_2,f)} \cdot x_{(p,l,f)}}{\beta_{(l,p,l,f)}^2 \cdot y_{(l,f)}} - x_{(p,l,f)} \right] \leq 1, \quad \forall p \in \mathcal{P}, l \in \mathcal{L}, f \in \mathcal{F} \quad (41)$$

TABLE 7
Main Notation.

	Symbol	Description	
Set Notation	\mathcal{P}	Set of pixels	
	$\mathcal{P}^{\text{RES}} \in \mathcal{P}$	Set of pixels in residential areas	
	$\mathcal{P}^{\text{GEN}} \in \mathcal{P}$	Set of pixels in general public areas	
	$\mathcal{P}^{\text{SENS}} \in \mathcal{P}$	Set of pixels in sensitive areas	
	\mathcal{L} \mathcal{F}	set of candidate locations for installing 5G gNBs Set of operating frequencies for 5G gNB	
Parameters	S_f^{MIN}	Minimum SIR to achieve in order to guarantee the required 5G service on frequency $f \in \mathcal{F}$	
	$\beta_{(l,p,l_2,f)}$	Signal/interference contribution from 5G gNB $l_2 \in \mathcal{L}$ on frequency $f \in \mathcal{F}$ over pixel $p \in \mathcal{P}$ served by gNB $l \in \mathcal{L}$	
	$C_{(l,f)}^{\text{SITE}}$	Site installation cost of a 5G gNB site operating on frequency $f \in \mathcal{F}$ at location $l \in \mathcal{L}$	
	C_f^{EQUIP}	Equipment cost of a 5G gNB operating on frequency $f \in \mathcal{F}$;	
	$P_{(p,f)}^{\text{BASE}}$	Baseline power density on frequency $f \in \mathcal{F}$ received by pixel $p \in \mathcal{P}$	
	$P_{(p,l,f)}^{\text{ADD}}$	Additional power density received by pixel $p \in \mathcal{P}$ from a 5G gNB installed at location $l \in \mathcal{L}$ operating on frequency $f \in \mathcal{F}$	
	L_f^{RES}	Power density limit over frequency $f \in \mathcal{F}$ for a pixel belonging to a residential area	
	L_f^{GEN}	Power density limit over frequency $f \in \mathcal{F}$ for a pixel belonging to a general public area	
	D^{MIN}	Minimum distance between an installed 5G gNB site and a sensitive place	
	D_f^{MAX}	Max. 5G coverage distance between a 5G gNB operating on frequency f and a covered pixel	
	$D_{(p,l,f)}$	Distance between pixel $p \in \mathcal{P}$ and a gNB operating on frequency $f \in \mathcal{F}$ and installed at location $l \in \mathcal{L}$	
	$I_{(p,l,f)}^{\text{ZONE}}$	Exclusion zone indicator: 1 if pixel $p \in \mathcal{P}$ falls inside the exclusion zone of a 5G gNB installed at location $l \in \mathcal{L}$ and operating on frequency $f \in \mathcal{F}$, 0 otherwise	
	N^{SER}	Maximum number of 5G gNBs that can serve a single pixel	
	N^{MAX}	Maximum number of 5G gNBs that can be installed in a location	
	$I_{(l,f)}^{\text{FREQ}}$	Indicator parameter: 1 if gNB operating on frequency $f \in \mathcal{F}$ can be installed at location $l \in \mathcal{L}$, 0 otherwise	
	$R_{(l,f)}^{\text{TIME}}$	Temporal scaling factor for a 5G gNB operating on frequency $f \in \mathcal{F}$ and installed at location $l \in \mathcal{L}$	
	$R_{(l,f)}^{\text{STAT}}$	Statistical scaling factor for a 5G gNB operating on frequency $f \in \mathcal{F}$ and installed at location $l \in \mathcal{L}$;	
	$\alpha_{(l,f)}$	Objective weight factor for the service coverage variables, depending on frequency $f \in \mathcal{F}$ and gNB location $l \in \mathcal{L}$.	
	Variables	$y_{(l,f)}$	5G gNB equipment binary variable: 1 if a 5G gNB equipment operating on frequency $f \in \mathcal{F}$ is installed at location $l \in \mathcal{L}$, 0 otherwise
		$x_{(p,l,f)}$	Binary 5G service variable : 1 if pixel $p \in \mathcal{P}$ is served by 5G gNB at location $l \in \mathcal{L}$ with frequency $f \in \mathcal{F}$, 0 otherwise
$P_{(p,f)}^{\text{ADD-TS}}$		Additional power density received by pixel $p \in \mathcal{P}$ from all the 5G gNBs operating on frequency $f \in \mathcal{F}$, computed over temporal and statistical scaling factors	
$P_{(p,f)}^{\text{ADD-NOTS}}$		Additional power density received by pixel $p \in \mathcal{P}$ from all the 5G gNB operating on frequency $f \in \mathcal{F}$, computed without temporal and statistical scaling factors	
w_p		Pixel in exclusion zone binary variable : 1 if pixel $p \in \mathcal{P}$ falls inside an exclusion zone of an installed 5G gNB, 0 otherwise	
C^{TOT}		Variable storing the total installation costs for the installed 5G gNBs.	

By recalling constraint (12), we know that $x_{(p,l,f)} = 1$ only if $y_{(l,f)} = 1$ (and both Eq. (12) and Eq. (13) are ensured). In other words, $x_{(p,l,f)}$ can not be set to 1 if the gNB operating on f is not installed in l , i.e., $y_{(l,f)} = 0$. As a result, the ratio $x_{(p,l,f)}/y_{(l,f)}$ can be simply expressed as $x_{(p,l,f)}$. Consequently, constraint (41) can be rewritten in the following equivalent form:

$$S_f^{\text{MIN}} \cdot \left[\sum_{l_2 \in \mathcal{L}} \frac{\beta_{(l,p,l_2,f)}^2}{\beta_{(l,p,l,f)}^2} \cdot y_{(l_2,f)} \cdot x_{(p,l,f)} - x_{(p,l,f)} \right] \leq 1, \quad \forall p \in \mathcal{P}, l \in \mathcal{L}, f \in \mathcal{F} \quad (42)$$

The previous constraint can be easily linearized by: *i*)

TABLE 8
Computational complexity of the routines and PLATEA algorithm

Procedure	Complexity
INITIAL_SOL	$\mathcal{O}(\mathcal{P} \times \mathcal{L} \times \mathcal{F})$
EXTRACT_SITES	$\mathcal{O}(N^{\text{COMB}})$
INSTALL_CHECK	$\mathcal{O}(\mathcal{P} \times \mathcal{L} \times \mathcal{F})$
ASSOCIATE_PIXELS	$\mathcal{O}(\mathcal{P} \times \mathcal{L} ^2 \times \mathcal{F})$
COMPUTE_OBJ	$\mathcal{O}(\mathcal{P} \times \mathcal{L} \times \mathcal{F})$
SAVE_SOL	$\mathcal{O}(\mathcal{P} \times \mathcal{L} \times \mathcal{F})$
INITIALIZE	$\mathcal{O}(\mathcal{P} \times \mathcal{L} \times \mathcal{F})$
ALL_SERVED	$\mathcal{O}(\mathcal{P} \times \mathcal{L} \times \mathcal{F})$
SELECT_BEST_SET_F1	$\mathcal{O}(N^{\text{COMB}} \times \mathcal{P} \times \mathcal{L} ^2 \times \mathcal{F})$
PLATEA	$\mathcal{O}(N^{\text{COMB}} \times \mathcal{P} \times \mathcal{L} ^4 \times \mathcal{F})$

introducing the binary auxiliary variable $v_{(l,p,l_2,f)} \in \{0,1\}$, *ii*) replacing (42) with the following set of constraints:

$$v_{(l,p,l_2,f)} \leq x_{(p,l,f)}, \quad \forall p \in \mathcal{P}, l \in \mathcal{L}, l_2 \in \mathcal{L}, f \in \mathcal{F} \quad (43)$$

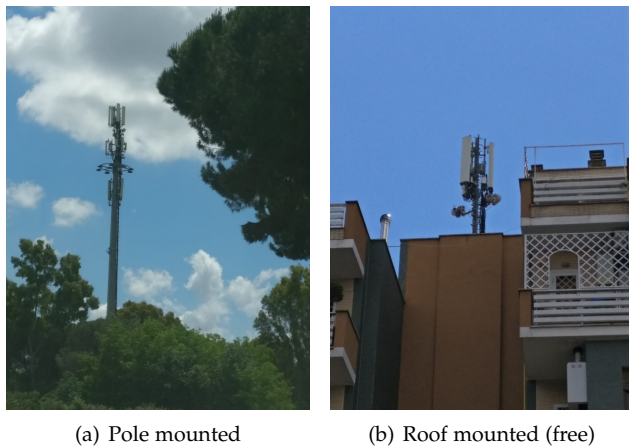
$$v_{(l,p,l_2,f)} \leq y_{(l_2,f)}, \quad \forall p \in \mathcal{P}, l \in \mathcal{L}, l_2 \in \mathcal{L}, f \in \mathcal{F} \quad (44)$$

$$v_{(l,p,l_2,f)} \geq x_{(p,l,f)} + y_{(l_2,f)} - 1, \quad \forall p \in \mathcal{P}, l \in \mathcal{L}, l_2 \in \mathcal{L}, f \in \mathcal{F} \quad (45)$$

$$S_f^{\text{MIN}} \cdot \left[\sum_{l_2 \in \mathcal{L}} \frac{\beta_{(l,p,l_2,f)}^2}{\beta_{(l,p,l,f)}^2} \cdot v_{(l,p,l_2,f)} - x_{(p,l,f)} \right] \leq 1 \quad \forall p \in \mathcal{P}, l \in \mathcal{L}, f \in \mathcal{F} \quad (46)$$

APPENDIX E PLATEA COMPUTATIONAL COMPLEXITY

Tab. 8 reports the computational complexity of the routines, functions and the whole PLATEA algorithm. Several considerations hold by analyzing the table. First, we denote with N^{COMB} the number of combinations that are generated by the EXTRACT_SITES routine. Second, the computational complexity of INSTALL_CHECK, ASSOCIATE_PIXELS and COMPUTE_OBJ are derived from the implementation of constraints Eq. (19), (20), (22)-(31), (12),(13), (15)-(18), (32), (33). Third, the whole computational complexity of PLATEA grows linearly with the number of pixels and with the number of frequencies. Fourth, although the complexity of PLATEA may appear substantially large at a first glance, due to the term $N^{\text{COMB}} \times |\mathcal{L}|^4$, we remind that the number of candidate sites $|\mathcal{L}|$ is rather limited in practice, due to the intrinsic difficulty in finding suitable locations that can host gNB equipment. In addition, in our work we constrain N^{COMB} to be in the same order of magnitude of $|\mathcal{L}|$. Therefore, overall complexity of PLATEA is in the order of $\mathcal{O}(|\mathcal{P}| \times |\mathcal{L}|^5 \times |\mathcal{F}|)$.



(a) Pole mounted

(b) Roof mounted (free)



(c) Roof mounted (hidden)

Fig. 10. Three examples of pre-5G Base Stations serving the TMC neighborhood.

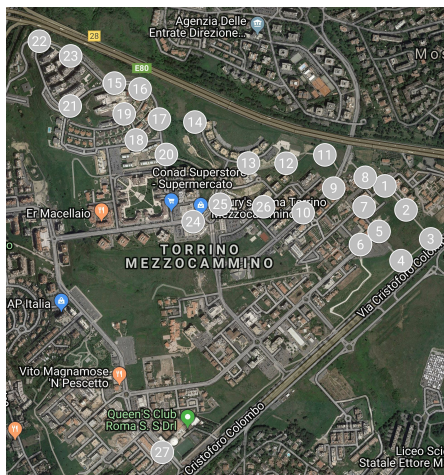
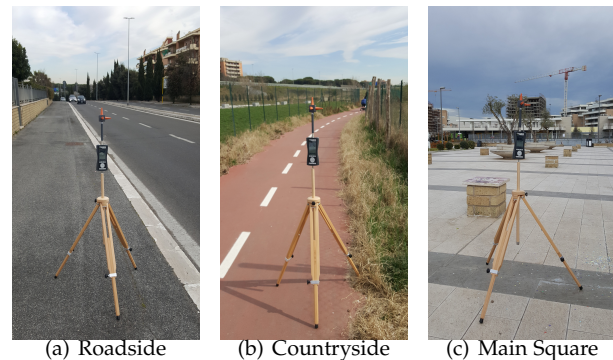


Fig. 11. Measurement locations in the TMC scenario.

APPENDIX F EMF MEASUREMENTS IN THE TMC SCENARIO

We describe here the methodology adopted to perform the EMF measurements in the TMC scenario, as well as the main outcomes from the measurements. Actually, the TMC neighborhood does not host any installation of legacy pre-5G Base Stations, mainly due to the following reasons: *i*) TMC is a relatively new neighborhood, which was built during the last decade and *ii*) all the requests done by operators to install Base Stations in the neighborhood have been denied by the municipality, since the selected locations



(a) Roadside

(b) Countryside

(c) Main Square

Fig. 12. Three examples of EMF measurement location in the TMC neighborhood.

did not ensure the minimum distance from the sensitive places. As a result, the cellular service over TMC is provided by a set of Base Stations installed in other neighborhoods. We refer the interested reader to Fig. 8 of [1] for the maps reporting the localization of pre-5G Base Stations serving TMC. In brief, these Base Stations include pole mounted and roof mounted installations (with some examples reported in Fig. 10), mainly close to the north-east and east borders of the neighborhood. Therefore, rather than measuring the EMF levels in each pixel of TMC neighborhood (which would require a huge amount of time), we concentrate on the TMC zones in close proximity to the Base Stations installed in the other neighborhoods, since these zones are expected to receive the highest EMF exposure levels. To this aim, Fig. 11 reports the considered measurement locations, each of them labelled with a unique ID. In addition, we place the EMF meter in outdoor locations and in general in zones not covered by obstacles. To this aim, Fig. 12 reports three examples of measurement locations, by differentiating between: roadside positioning (Fig 12(a)), countryside positioning (Fig. 12(b)), and positioning in the main square (Fig. 12(c)).

In the following, we measure the electric field in each measurement point, by adopting a professional EMF meter, whose settings are detailed in Tab. 9. More in depth, the meter provides the total electric field over the set of frequencies used by cellular operators. In addition, all the measurements have been performed during morning/afternoon hours of business days. In this way, the measured electric field is retrieved under moderate/high utilization of the cellular network. In addition, we consider the value of 6 [min] as the reference time interval to compute the average electric field (in accordance to regulation R1 of Tab. 3). Although Italian regulations integrate longer time-intervals to compute the average electric field (see e.g., R3-R4 of Tab. 3), we believe that the considered scenario is rather conservative, since the measurements are performed during moderate/high utilization of the cellular network, and hence during time intervals during which the electric field is higher compared to low traffic conditions (e.g., at night, during holidays, during week-ends).

Fig. 13 reports the average EMF levels over the measurement locations. Several considerations hold by analyzing the figure. First, the average electric field is always pretty low,

Algorithm 3 Pseudo-Code of the EVALUATION ALGORITHM (EA)

Input: num_f1 of deployed gNBs with frequency f_1 , num_f2 of deployed gNBs with frequency f_2
Output: flag_check flag with installation status (true = installation successful, false = installation unsuccessful), variables $y, x, P^{\text{ADD-TS}}, P^{\text{ADD-NOTS}}, w, C^{\text{TOT}}$

```

1: cand_sites=GENERATE_SITES(num_f1,num_f2); // Random generation of a candidate deployment
2: [x_temp y_temp pd_temp]=INITIALIZE(cand_sites);
3: [flag_check, pd_temp]=INSTALL_CHECK(cand_sites, y_temp, pd_temp); // Based on Eq. (19), (20), (22)-(31)
4: if flag_check==true then
5:   [x_temp]=ASSOCIATE_PIXELS(y_temp,x_temp); // Based on Eq. (12), (13), (15)-(18)
6:   [y, x, P^ADD-TS, P^ADD-NOTS, w, C^TOT]=SAVE_SOL(y_temp, x_temp, pd_temp); // Solution saving
7: end if

```

Algorithm 4 Pseudo-Code of the MAXIMUM COVERAGE MACRO ALGORITHM (MCMA)

Input: num_f1 of deployed gNBs with frequency f_1
Output: flag_sol flag with installation status (true = feasible solution found, false = no feasible solution found), variables $y, x, P^{\text{ADD-TS}}, P^{\text{ADD-NOTS}}, w, C^{\text{TOT}}$

```

1: num_f2_max= $\sum_{l \in \mathcal{L}} I_{(f_2,l)}^{\text{FREQ}}$ ;
2: flag_end=false;
3: flag_sol=false;
4: num_f2=1;
5: while flag_end==false do
6:   cand_sites=GENERATE_SITES(num_f1,num_f2); // Random generation of a candidate deployment
7:   [x_curr y_curr pd_curr]=INITIALIZE(cand_sites);
8:   [flag_check, pd_curr]=INSTALL_CHECK(cand_sites, y_curr, pd_curr); // Based on Eq. (19), (20), (22)-(31)
9:   if flag_check==true then
10:    [x_curr]=ASSOCIATE_PIXELS(y_curr,x_curr); // Based on Eq. (12), (13), (15)-(18)
11:    flag_sol=true;
12:   end if
13:   if (ALL_SERVED(x_curr)==true) or (num_f2==num_f2_max) then
14:     if flag_check==true then
15:       [y, x, P^ADD-TS, P^ADD-NOTS, w, C^TOT]=SAVE_SOL(y_curr, x_curr, pd_curr); // best Solution Saving
16:     end if
17:     flag_end=true; // Stop condition
18:   else
19:     num_f2++;
20:   end if
21: end while

```

H.1 EA Description

Alg. 3 reports the EA pseudo-code. This algorithm takes as input the number of deployed gNBs over the two frequencies, which are stored in the num_f1 and num_f2 parameters. EA then returns as output a warning flag, which is set to false if the installation have been unsuccessful (due to the fact the constraints are not ensured), true otherwise. In addition, the information about the obtained planning is returned in the $y, x, P^{\text{ADD-TS}}, P^{\text{ADD-NOTS}}, w, C^{\text{TOT}}$ variables. Initially (line 1), EA generates a random deployment with num_f1 f_1 gNBs and num_f2 f_2 gNBs. In the following, EA initializes a set of internal variables (line 2). Then, EA performs in line 3 the feasibility checks of: *i*) power density limits outside exclusion zones, *ii*) minimum distance from sensitive places, *iii*) maximum number of gNBs installed in each site and *iv*) site installation constraints. If all these constraints are ensured (line 4), EA performs the pixel-gNB association (by first iterating over the f_1 gNBs and then over the f_2 gNBs) and then the solution is saved (lines 5-6).

Computational Complexity. The GENERATE_SITES function has a complexity of $\mathcal{O}(|\mathcal{L}|)$. The complexity of INITIALIZE, INSTALL_CHECK, ASSOCIATE_PIXELS and SAVE_SOL is reported in Tab. 8. Therefore, the total computational complexity of EA is in the order of $\mathcal{O}(|\mathcal{P}| \times |\mathcal{L}|^2 \times |\mathcal{F}|)$.

H.2 MCMA Description

Alg. 4 reports the pseudo-code of MCMA algorithm. The algorithm requires as input the number of f_1 gNBs to be installed. MCMA then produces as output a flag, indicating if a feasible solution has been found, and the problem variables $y, x, P^{\text{ADD-TS}}, P^{\text{ADD-NOTS}}, w, C^{\text{TOT}}$. The main intuition behind MCMA is to sequentially iterate over the number of f_2 gNBs to be installed, i.e. from 1 up to num_f2_max (lines 5-21). In particular, MCMA generates the set of candidate gNBs from num_f1 and num_f2 (line 6), initializes the variables (line 7), runs the INSTALL_CHECK function (line 8) and eventually associates the pixels to the installed gNBs (line 10). The iteration stops if all the pixels have been served or the maximum number of f_2 gNBs have been evaluated (line 13). Under this condition, the current solution is eventually saved and the algorithm is ended (lines 14-17). Otherwise, the current number of f_2 gNB is increased (line 18) and lines 5-21 are evaluated again.

Computational complexity. The functions employed by MCMA are the ones also used by EA (detailed in Sec. H.1) and PLATEA (detailed in Tab. 8). In addition, the while cycle in line 5 has a complexity of $\mathcal{O}(|\mathcal{L}|)$. Therefore, the total complexity of MCMA is in the order of $\mathcal{O}(|\mathcal{P}| \times |\mathcal{L}|^3 \times |\mathcal{F}|)$.

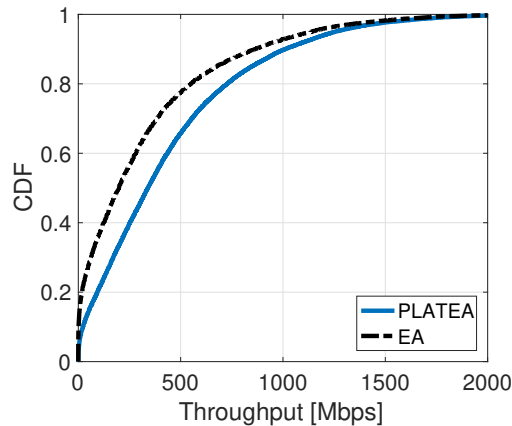


Fig. 15. CDF of the pixel throughput T_p obtained by PLATEA and EA.

APPENDIX I ADDITIONAL RESULTS

In this section, we provide a set of additional results, in order to better position the PLATEA algorithm and the results presented in Sec. 7.

I.1 Throughput Comparison

Tab. 6 in Sec. 7 highlights that PLATEA achieves a better average throughput T^{AVG} compared to EA and MCMA. However, no indication about the throughput of the single pixels (which we remind is denoted with T_p) is provided. Therefore, a natural question is: which is the performance of PLATEA when considering T_p and not T^{AVG} ? To answer this question, Fig. 15 reports the Cumulative Distribution Function (CDF) of the throughput T_p obtained with PLATEA. In addition, the figure shows the CDF obtained by running EA. Three considerations hold by analyzing Fig. 15. First, PLATEA is able to guarantee more than 500 [Mbps] of throughput for more than 25% of pixels. Second, the percentage of pixels receiving very low throughput is overall pretty limited (less than 10%). Third, EA performs consistently worse, being its CDF clearly moved on the left w.r.t. PLATEA.

I.2 Number of f_2 gNBs selected by MCMA

According to Tab. 6 in Sec. 7, MCMA requires a consistently higher amount of f_2 gNBs compared to PLATEA. However, a natural question is: Does MCMA always install more f_2 gNBs w.r.t. PLATEA? To answer this question, we run MCMA by varying num_f1 between 1 and 24 (which corresponds to the maximum number of gNB installed by PLATEA for very large values of $\alpha_{(l,f1)}$). For each value of num_f1 , we then perform 10 executions of MCMA, and then we collect the average number of installed f_2 gNBs over the 10 runs. Fig. 16 reports the variation of the average number of installed f_2 gNBs vs. num_f1 . For completeness, the figure reports also the number of f_2 gNBs that are installed by PLATEA. Interestingly, we can note that the average number of installed f_2 gNBs is always higher than the one selected by PLATEA. This difference may be explained in the different planning policies adopted by the two solutions. MCMA, in fact, sequentially evaluates

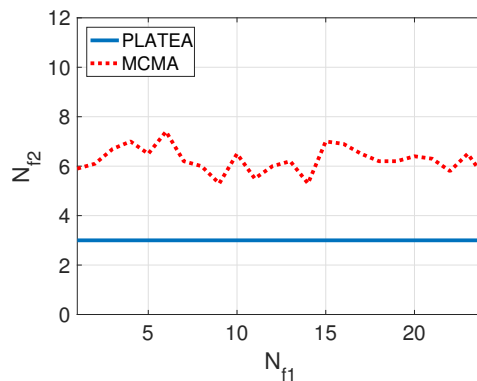


Fig. 16. Number of f_2 gNBs installed by PLATEA and MCMA for different numbers of f_1 gNBs.

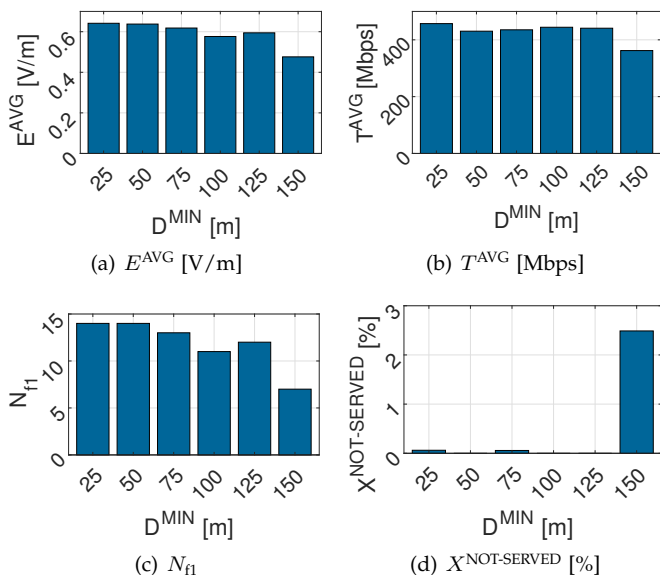


Fig. 17. Impact of D^{MIN} variation on: i) average electric field E^{AVG} , ii) average throughput T^{AVG} , iii) number N_{f1} of f_1 gNBs and iv) percentage of not served pixels $X^{NOT-SERVED}$.

an increasing number of f_2 gNB, given the number of f_1 gNBs that is passed as input parameter. On the other hand, PLATEA operates a wiser choice, by: i) evaluating a number of combinations that increases with the number of gNBs that need to be installed, and ii) jointly varying the number of f_1 gNB and f_2 gNB when evaluating the problem constraints and the objective function.

I.3 Impact of minimum distance constraint

The set of regulations taken under consideration in this work (namely $R6$ of Tab. 3) includes a minimum distance D^{MIN} between each installed gNBs and each sensitive place. A natural question is then: What is the impact of D^{MIN} variation on the planning? To answer this question, we have assumed that D^{MIN} can take different values w.r.t. the ones reported in the regulations. In particular, we have considered the following range of values for $D^{MIN} = \{25, 50, 75, 100, 125, 150\}$. We have then run PLATEA algorithm for each D^{MIN} value, and we have collected the performance metrics. Fig. 17 reports the obtained

TABLE 10
PLATEA performance vs. different pre-5G exposure terms.

Metric	Pre-5G Exposure		
	1.0 [V/m]	1.5 [V/m]	2.0 [V/m]
C^{TOT} [k€]	371.9	343.3	267.9
N_{f1}	9.9	7.9	4
N_{f2}	3	3.1	3
X_{f1}^{SERVED}	8779	7409	4501
X_{f2}^{SERVED}	15534	16869	19789
$X^{\text{NOT-SERVED}}$ [%]	0.01	0.16	0.11
T^{AVG} [Mbps]	429.99	411.74	374.42
E^{AVG} [V/m]	1.18	1.62	2.06

results in terms of: *i*) average electric field E^{AVG} , *ii*) average throughput T^{AVG} , *iii*) number N_{f1} of $f1$ gNBs and *iv*) percentage of not served pixels $X^{\text{NOT-SERVED}}$. We remind that $D^{\text{MIN}} = 100$ [m] is the value currently enforced in the Rome regulations. Interestingly, when $D^{\text{MIN}} < 100$ [m], E^{AVG} , T^{AVG} and N_{f1} tend to be increased, due to the fact that it is possible to install more gNBs over the territory while ensuring the minimum distance constraint. On the other hand, the opposite holds $D^{\text{MIN}} > 100$ [m]. In particular, when $D^{\text{MIN}} = 150$ [m], an abrupt decrease of E^{AVG} , T^{AVG} and N_{f1} is observed. These results are a direct consequence of the D^{MIN} , which prevents the installation of gNBs in many TMC locations. In addition, the setting of $D^{\text{MIN}} = 150$ [m] is also detrimental for UE, since the percentage of not served pixels is abruptly increased to more than 2%. Therefore, we can conclude that the variation of D^{MIN} affects the selected planning, especially for values larger than 100 [m].

I.4 Impact of pre-5G exposure levels

The goal of this part is to study the impact of adding the pre-5G exposure term on the 5G planning. As detailed in Appendix F, the actual electric field strength in TMC hardly exceeds 1 [V/m], even for the pixels that are at the shortest distance and Line-of-Sight (LOS) conditions w.r.t. the serving gNB. On the other hand, the electric field rapidly decreases to negligible values (below 1 [V/m]) as the distance between the pixel and the radiating gNBs increases. However, in order to introduce a set of conservative (and worst case) scenarios, we assume: *i*) three different settings of pre-5G exposure, namely 1 [V/m], 1.5 [V/m] and 2 [V/m], and *ii*) a uniform term of pre-5G exposure for all the pixels in the TMC scenario.²¹ As a consequence, the cumulative pre-5G power density is set as $\sum_{f \in \mathcal{F}} P_{(p,f)}^{\text{BASE}} = \{0.00265, 0.00597, 0.0106\}$ [W/m²], $\forall p \in \mathcal{P}$, respectively. In addition, since the same restrictive limit is applied for all the pixels of TMC, Eq. (27) is rewritten as:

$$(1-w_p) \cdot \underbrace{\sum_{f \in \mathcal{F}} P_{(p,f)}^{\text{BASE}}}_{\text{pre-5G Exposure Term}} + \underbrace{\sum_{f \in \mathcal{F}} P_{(p,f)}^{\text{ADD-TS}}}_{\text{5G Exposure Term}} \leq L^{\text{RES}}, \quad \forall p \in \mathcal{P}^{\text{RES}} \quad (48)$$

21. The application of a background exposure of 2 [V/m] is equivalent to the case in which the limit L^{RES} equal to 4 [V/m], a value currently in use in many Swiss cantons and in Monaco. Alternatively, the background exposure can be also seen as a margin that is left for the deployment of post-5G networks.

TABLE 11
Impact of the frequency reuse scheme $\epsilon_f^{\text{F-REUSE}}$ on PLATEA.

Metric	$\epsilon_f^{\text{F-REUSE}} = 1$	$\epsilon_f^{\text{F-REUSE}} = 3$	$\epsilon_f^{\text{F-REUSE}} = 7$
C^{TOT} [k€]	386.1	354.3	320.2
N_{f1}	10.7	8.9	7
N_{f2}	3	3	3
X_{f1}^{SERVED}	9103	7465.3	5999.5
X_{f2}^{SERVED}	15307	16845.3	18305.3
$X^{\text{NOT-SERVED}}$ [%]	0.03	0.03	0.05
T^{AVG} [Mbps]	428.3	144.1	60.4
E^{AVG} [V/m]	0.57	0.53	0.48

where $L^{\text{RES}} = 0.1$ [W/m²] (in accordance to R6 of Tab. 3). Intuitively, the introduction of the pre-5G exposure term may limit the amount of 5G gNBs that are installed over the territory, since it is more challenging to ensure Eq. (48) compared to the case in which the pre-5G technologies are dismissed.

Tab. 10 reports the performance metrics of PLATEA (averaged over 10 runs) vs. the different values of pre-5G exposure. When the pre-5G exposure is increased, we can note: *i*) a reduction in the number of $f1$ gNBs, and consequently of total costs, *ii*) an increase in the number of pixels served by $f2$ gNBs, *iii*) a throughput decrease, and *iv*) an EMF increase, mainly due to the pre-5G exposure term. Overall, these results prove that the performance metrics are impacted by the level of background exposure. However, PLATEA is always able to retrieve a feasible planning, with a percentage of unserved pixels at most equal to 0.16%.

I.5 Impact of frequency reuse scheme

Finally, we have considered the case in which the frequency reuse is different than unity. More formally, the frequency reuse factor can be easily changed by varying the value of $\epsilon_f^{\text{F-REUSE}}$, which appear in Eq. (3), and therefore in the throughput metrics reported in Tab. 5. In the following, we consider the following variation of frequency reuse scheme: $\epsilon_f^{\text{F-REUSE}} = \{1, 3, 7\}$ (for both $f1$ and $f2$). In addition, we adopt the conservative assumption that the change of $\epsilon_f^{\text{F-REUSE}}$ does not affect the SIR computation in Eq. (1).²²

Tab. 11 reports the main metrics when PLATEA solves the TMC scenario under 1, 3, and 7 frequency reuse schemes (with values averaged over 10 independent runs). As expected, the increase of $\epsilon_f^{\text{F-REUSE}}$ notably reduce the throughput T^{AVG} . In particular, since it is more challenging to ensure the minimum traffic constraint for the micro gNBs, PLATEA tends to associate more pixels to the macro gNBs. Consequently, the number of micro gNBs is decreased, and therefore the overall costs C^{TOT} are reduced. This is in turn beneficial for the average EMF levels E^{AVG} , which pass from 0.57 [V/m] when $\epsilon_f^{\text{F-REUSE}} = 1$ to 0.48 [V/m] when $\epsilon_f^{\text{F-REUSE}} = 7$.

22. Intuitively, the SIR may be improved when the frequency reuse scheme is increased, because a lower number of interfering gNBs are counted in the SIR denominator of Eq. (1). We refer the reader to [13] for a thorough analysis of this aspect. In this work, we consider a worst-case scenario, in which the increase of $\epsilon_f^{\text{F-REUSE}}$ reduces the available bandwidth of Eq. (3), while the SIR in Eq. (1) is not improved.